

Effect of Mechanical Entrapment on Efficiency of Polymer Enhanced Oil Recovery



Department of Environment, Land and Infrastructure Engineering

Supervisors:

Dr. Vera Rocca

Dr. Rouhi Farajzadeh

Prof. Hans Bruining

Dr. Bernhard Meulenbroek

Author :

Ramin Soltanmohammadi

October 2019

Thesis submitted in compliance with the requirements for the Master of Science degree

TABLE OF CONTENTS

CHAPTER 1 INTRODUCTION	1
1.1 RESEARCH OVERVIEW.....	2
1.2 PROJECT OBJECTIVE	2
1.3 OUTLINES OF CHAPTERS	3
CHAPTER 2 THEORETICAL BACKGROUND AND LITERATURE REVIEW	5
2.1 GENERAL INTRODUCTION TO EOR METHODS.....	6
2.2 POLYMER	8
2.3 POLYMER FLOODING MECHANISMS	8
2.3.1 <i>Mobility Ratio</i>	9
2.3.2 <i>Sweep Efficacy</i>	14
2.4 POLYMER RETENTION.....	15
CHAPTER 3 PHYSICS AND MATHEMATICS	18
3.1 MASS CONSERVATION:.....	19
3.2 PARTIAL DIFFERENTIAL EQUATIONS	22
3.3 SUMMARY OF EQUATIONS AND BOUNDARY CONDITIONS	29
3.4 MECHANICAL ENTRAPMENT AND ADSORPTION	31
CHAPTER 4 NUMERICAL SIMULATION	35
4.1 WATER FLOODING.....	36
4.2 POLYMER FLOODING	40
4.2.1 <i>Single phase flow</i>	40
4.2.2 <i>Two phase flow</i>	44
4.3 EFFECT OF MECHANICAL ENTRAPMENT IN 2D MODEL:.....	56
CHAPTER 5 CONCLUSION	58
CHAPTER 6 BIBLIOGRAPHY	61

TABLE OF FIGURES

FIGURE 1 : EOR METHODS, APPLICATIONS, AND RECOVERY RATE (DALEEL PRTEOLEUM L.L.C.) (THOMAS, 2008)....	7
FIGURE 2 : MONOMER AND POLYMER (USUALLY POLYMER WHICH USED IN EOR CONTAINS AT LEAST EIGHT CONNECTED MONOMERS CHAINS) (UNSW, SCHOOL OF MATERIAL SCIENCE AND ENGINEERING , 2013).....	8
FIGURE 3: WATER SATURATION PROFILE DURING POLYMER FLOODING. TWO SATURATION SHOCK FRONTS WILL REPRESENT DURING POLYMER EOR, THE FIRST FRONT REPRESENTS THE BOUNDARY BETWEEN FLUID-IN-PLACE AND WATER. WHILE THE SECOND FRONT REPRESENTS THE BOUNDARY BETWEEN POLYMER AND OIL-BANK. THE DASH LINE SHOWS THE POLYMER CONCENTRATION. AFTER THE SECOND SHOCK WE DO NOT HAVE ANY CHEMICALS. (BOUQUET, 2017)	11
FIGURE 4 : FRACTIONAL FLOW AND DIMENSIONLESS LENGTH VS. WATER SATURATION, THE FIRST AND SECOND SHOCK FRONT VELOCITY CAN ACHIEVE USING THE FOLLOWING METHOD. POINT "J" REPRESENTS THE INJECTION SITUATION AND POINT "I" DISPLAYS THE INITIAL CONDITION. (FARAJZADEH, 2019)	12
FIGURE 5: (A) FRACTIONAL FLOW DIAGRAM (WITH POLYMER ADSORPTION), (B) SATURATION PROFILE DURING POLYMER FLOODING (POPE, 1980)	13
FIGURE 6: POLYMER ADSORPTION VS. POLYMER CONCENTRATION. ORDINARILY, BY INCREASING THE POLYMER CONCENTRATION, THE ADSORPTION POLYMER WILL INCREASE. (ZHANG, 2014)	13
FIGURE 7: VERTICAL SWEEP EFFICIENCY OF WATER VS POLYMER FLOODING (PRASAD, 2018).....	14
FIGURE 8: AREAL SWEEP EFFICIENCY OF WATER VS POLYMER FLOODING (PRASAD, 2018)	15
FIGURE 9 : POLYMER RETENTION IN POROUS MEDIA (LAKE, 2014)	16
FIGURE 10 : FIELD BHP AND INJECTION RATE (LOTFOLLAHI M. , 2015).....	16
FIGURE 11: DISTRIBUTION OF POLYMER MOLECULE SIZE AND ROCK PORE SIZE (LOTFOLLAHI M. , 2016).....	17
FIGURE 12 : MASS EXCHANGE IN A DEFINED SECTION WITH VOLUME "V".	19
FIGURE 13: THE BLUE LINES IN THIS FIGURE SHOWS THE ZERO FLUX. WHICH MEANS THAT WE DO NOT HAVE ANY FLOW FROM THESE BOUNDARIES.	30
FIGURE 14: WATER SATURATION VS. LENGTH IN HOMOGENEOUS RESERVOIR AT 0.17 PORE VOLUME INJECTED (PV), 0.28 PV, 0.32 PV AND 0.55 PV WHICH REPRESENT THAT WATER SATURATION AT UPSTREAM SHOCK IS 0.37 AND AT THE DOWNSTREAM IS 0.2.	36
FIGURE 15: OIL AND WATER RELATIVE PERMEABILITY VS. WATER SATURATION USING COREY-TYPE FUNCTION	37
FIGURE 16: WATER FLOODING IN RESERVOIR AND VISCOUS FINGERING DUE TO HIGH MOBILITY RATIO (MOBILITY RATIO ABOVE 1)	38
FIGURE 17: WATER FLOODING WITH THE FAVORABLE MOBILITY RATIO, SO THE VISCOSE FINGERING DISAPPEARED AND WATER SHOCK FRONT IS STABLE.	40
FIGURE 18 : THE POLYMER CONCENTRATION FOR A CASE WE DO NOT HAVE ADSORPTION. MECHANICAL ENTRAPMENT DECREASES THE POLYMER CONCENTRATION AT THE SATURATION SHOCK FRONT.....	41
FIGURE 19: DIMENSIONLESS TRAPPED POLYMER CONCERTATION IN CASE WE HAVE CONSTANT FILTRATION COEFFICIENT. (THE POLYMER ADSORPTION NEGLECTED IN THIS FIGURER)	42
FIGURE 20 : PROPAGATION OF POLYMER IN POROUS MEDIA IS MAINLY RELY ON MECHANICAL ENTRAPMENT. IN THIS FIGURE B= 10 (LANGMUIR POLYMER ADSORPTION PARAMETER), AND MAXIMUM DIMENSIONLESS ADSORBED POLYMER CONCENTRATION IS 0.5 ($C_{max} = 0.5$), AND DIMENSIONLESS FILTRATION COEFFICIENT IS 2 ($\Lambda = 2$).	43
FIGURE 21: THE ADSORPTION DATA IN EXACTLY SAME AS FIGURE 18. HOWEVER IN THIS CASE THE DIMENSIONLESS FILTRATION COEFFICIENT DECREASES TO 0.5 ($\Lambda = 0.5$)......	43
FIGURE 22: OUTLET POLYMER CONCENTRATION VS. PORE VOLUME INJECTED. THE DIFFUSION COEFFICIENT EFFECT REPRESENTED IN THE FIGURE (BY DECREASING DIFFUSION COEFFICIENT DISPERSION OF CONCENTRATION INCREASES AND MODEL HAS BETTER MATCH WITH EXPERIMENTAL DATA. HOWEVER ANALYTICAL SOLUTION MATCHED WITH BLUE LINE)	44
FIGURE 23: THE POLYMER FLOODING, WITHOUT ADSORPTION AND MECHANICAL ENTRAPMENT. THE MOBILITY RATIO IS ABOUT 1. AND THE POLYMER VISCOSITY ID 8 cP. THEREFORE, WE DO NOT HAVE ANY VISCOUS FINGERING OR INSTABILITY IN THIS CASE. THE INSTABILITY REPRESENTED IN LAST TIME STEPS IS DUE TO LOW AMOUNT OF DIFFUSION COEFFICIENT, SO IT IS NUMERICAL ISSUE. TIME STEPS HERE IS 0.05 PORE VOLUME INJECTED.	45
FIGURE 24: THIS FIGURES REPRESENTS THE WATER SATURATION AND THE POLYMER CONCENTRATION IN THE CASE THAT THE POLYMER-SOLUTION VISCOSITY ID 6 cP. THEREFORE, COMPARE WITH THE PREVIOUS CASE THE WATER	

SATURATION AT THE OIL-BANK WILL DECREASES, THE MOBILITY RATIO INCREASES AND THE POLYMER CONCENTRATION REMAINS CONSTANT. BECAUSE IN THESE TWO WE DO NOT HAVE ADSORPTION OR MECHANICAL ENTRAPMENT OF THE POLYMER. THEREFORE THE DIMENSIONLESS POLYMER CONCENTRATION IS 1, AND AFTER POLYMER FRONT IT DROP RAPIDLY TO ZERO. 46

FIGURE 25: POLYMER FLOODING IN CASE WE HAVE MECHANICAL ENTRAPMENT IN POROUS MEDIA. THEREFORE, THE CONCENTRATION OF THE POLYMER AS IT REPRESENTED IN THE FIGURE WILL DROP, AS A FUNCTION OF PORE VOLUME INJECTED OR TIME. AS A RESULT, THE MOBILITY RATIO WILL INCREASE. IN THIS CASE WE USED $\lambda_0 = 0.4381m$ 48

FIGURE 26: IN CASE WE HAVE MECHANICAL ENTRAPMENT, THE MOBILITY RATIO INCREASED BY TIME (PV INJECTED) WHICH MEANS THAT THE CONCENTRATION OF POLYMER DECREASES CONSTANTLY AND REDUCTION OF POLYMER CONCENTRATION LEADS TO HAVE MORE MOBILITY RATIO. 49

FIGURE 27: IN CASE WE INCREASE THE POLYMER CONCENTRATION IN POLYMER-SOLUTION, WE CAN CONTROL EFFECT OF POLYMER ENTRAPMENT. AS IT REPRESENTED IN WATER SATURATION AND POLYMER CONCENTRATION FIGURES. 49

FIGURE 28: MOBILITY RATIO INCREASING DURING POLYMER FLOODING IN CASE WE HAVE MECHANICAL ENTRAPMENT. 50

FIGURE 29: HETEROGENEITY FIELD WHICH WE USED IN 2D MODEL. IN ORDER TO MONITOR VISCOUS FINGERING IN OUR SYSTEM BETTER WITH CONSIDERING THE $vdp=0.1$. WHICH IMPLIES THAT WE HAVE VISCOUS FINGERING NOR CHANNELING IN OUR NUMERICAL SIMULATION. 52

FIGURE 30: POLYMER FLOODING IN POROUS MEDIA IN CASE WE HAVE MOBILITY RATIO OF 2.17 IN POLYMER SATURATION SHOCK FRONT. AS REPRESENTED HERE WE CAN MONITOR INSTABILITY IN POLYMER SHOCK FRONT. 54

FIGURE 31: FRACTIONAL FLOW AS A FUNCTION OF WATER SATURATION. BLUE CURVE REPRESENTS THE POLYMER FLOODING IN POROUS MEDIA WHILE THE GREEN LINE DESCRIBES THE WATER FLOODING. IN CHAPTER 2, I EXPLAINED COMPLETELY HOW WE CAN OBTAIN WATER SATURATION IN UPSTREAM AND DOWNSTREAM THROUGH FRACTIONAL FLOW CURVES. 54

FIGURE 32: POLYMER PROPAGATION IN POROUS MEDIA WITH THE DATA AT TABLE 2. IN THIS CASE THE POLYMER VISCOSITY IS 7.2 cP. WHICH MEANS THAT THE MOBILITY RATIO IS 1. COMPARE WITH FIGURE 30, WHERE THE MOBILITY RATIO IS 2.17, WE CAN SHOWS THE EFFECT OF MOBILITY RATIO AND INSTABILITY OF POLYMER SHOCK FRONT. 55

FIGURE 33: USING EXACTLY THE SAME DATA WHICH WE HAVE IN TABLE 3 BUT WITH CONSIDERING MECHANICAL ENTRAPMENT. (ON THAT CASE WITHOUT CONSIDERING THE MECHANICAL ENTRAPMENT, THE MOBILITY RATIO WAS 1). HOWEVER IN THIS FIGURES WE CONSIDER EFFECT OF MECHANICAL ENTRAPMENT AND AS IT REPRESENTED WE HAVE INSTABILITY IN POLYMER SHOCK FRONT. ($\lambda_0 = 0.4381m, \sigma_{max} = 0.695, PECLT=9E10,$) 57

TABLES

TABLE 1: MOBILITY RATIO EFFECT ON AREAL SWEEP EFFICIENCY (AHMED, 2012).....	15
TABLE 2 : DATA USED FOR CONVENTIONAL WATER FLOODING IN BOTH HETEROGENEOUS AND HOMOGENEOUS RESERVOIRS	36
TABLE 3: INSERT DATA IN THE MODEL WITH CONSIDERING NO MECHANICAL ENTRAPMENT AND NO ADSORPTION IN POROUS MEDIA. THE POLYMER VISCOSITY IS 8 CP AND THE DATA OF TABLE 2 USED IN THIS MODEL	45
TABLE 4: IN THE POLYMER VISCOSITY 6CP AND TIME STEP 0.05 PORE VOLUME INJECTED (PV)	46
TABLE 5: THESE DATA USED FOR MODEL THE MECHANICAL ENTRAPMENT IN POROUS MEDIA. WE DO NOT CONSIDER ADSORPTION IN THIS SIMULATION.	47
TABLE 6: THE MOBILITY INCREASES AND IT IS FUNCTION OF PV. IN CASE WE DO NOT HAVE POLYMER RETENTION THE MOBILITY AT THE SAME CONDITION IS BELOW ONE. HOWEVER, IN THIS CASE THE MOBILITY RATIO RAISED UP AND WE HAVE INSTABLE SITUATION. THE “M” AND “N” WHICH IS USED IN THIS MODEL (ACCORDING TO EQUATION 56) ARE 10.3 AND 1.	48
TABLE 7: MOBILITY RATIO CALCULATION THROUGH WATER SATURATION AND POLYMER CONCENTRATION, POLYMER VISCOSITY, VARIATION.....	50

Chapter 1 *Introduction*

Enhanced oil recovery is the utilization of various technologies and methods to raise the volume of crude oil that can be generated from a reservoir. Polymer flooding is acknowledged as a chemical EOR method that promotes sweep efficiency by minimizing the mobility ratio, which is defined as a ratio among displaced and displacing fluids mobility. principally polymer does not affect remaining oil saturation. To decrease residual oil saturation ordinarily surfactant, add to the injected fluid to minimize interfacial tension (IFT). In this Thesis, we only concentrate on polymer EOR.

1.1 Research Overview

Polymer improves the areal and vertical sweep efficiency. The propagation of polymer executes a crucial task in performing polymer EOR. Chiefly, degradation and polymer retention are regarded as the most notable concerns that can influence polymer distribution. Polymer retention is mainly subdivided into polymer adsorption and mechanical entrapment. Polymer adsorption illustrates, polymer molecules adhere to the surface of the rock. Hence, the effective permeability diminished, and retardation happens at the polymer shock front. Mechanical entrapment belongs to the variation between the size of the polymer and the size of the pore throats. When the polymer diameters are larger than the smallest pore throats, the polymer captures the pores and decreases the effective permeability.

1.2 Project Objective

Polymer combines to water to enhance water viscosity. When the water viscosity raises the mobility ratio drops and it can aid in improving sweep efficiency. The polymer must propagate properly in porous media to have a desirable sweep efficiency. Polymer distribution predominantly refers to polymer retention. Polymer retention is divided into adsorption and mechanical plugging.

Adsorption means polymer adsorbs on the surface of the rock. The velocity of the polymer current reduces. Adsorption admitted as an irreversible phenomenon, generate a decline in polymer concentration and effective permeability. After a feasible long period of polymer injection, adsorption comes to the richest value. After that, the concentration of the polymer in the inlet and outlet must be equivalent. However, experiments show that the polymer concentration in the outlet is lower than the injected one. The pressure in the inlet rises continuously. The inlet pressure is a function of time during polymer flooding. It exhibits the effect of polymer entrapment, neither adsorption. Because of mechanical entrapment, polymers that have higher diameters compared with the narrowest pore throats in porous media will trap. As a result, polymer concentration reduces at the saturation shock front. Plus, effective permeability also decreases, which is the main element for the gradual increases in pressure in the inlet after a reasonable long injection. The most notable importance of the rise of pressure in inlet shows up when we examine operation limitations that we have during polymer injection. Well-injectivity decreases when we have mechanical entrapment. Further, reducing the mechanical entrapment can lessen the polymer concentration at the polymer shock front, and as a result, the mobility ratio rises. In this research, we investigate the effect of polymer entrapment and adsorption on the instability of the shock front. We examine the effect of mechanical entrapment and adsorption on mobility alteration at the shock front. To compensation mobility reduction and have a stability in the shock front, how polymer concentration must adapt.

1.3 Outlines of Chapters

This thesis comprises a theoretical and literature review in Chapter 2, covering an overview of polymer EOR mechanisms and previous research on polymer retention and adsorption. In Chapter 3, all the equations required to model polymer retention and implemented in the COMSOL code

are described. In Chapter 4, the results of the numerical simulation and the impression of polymer adsorption and mechanical entrapment are represented. The final chapter exhibits the conclusions for this project and recommendations for future projects.

Chapter 2 *Theoretical Background And Literature Review*

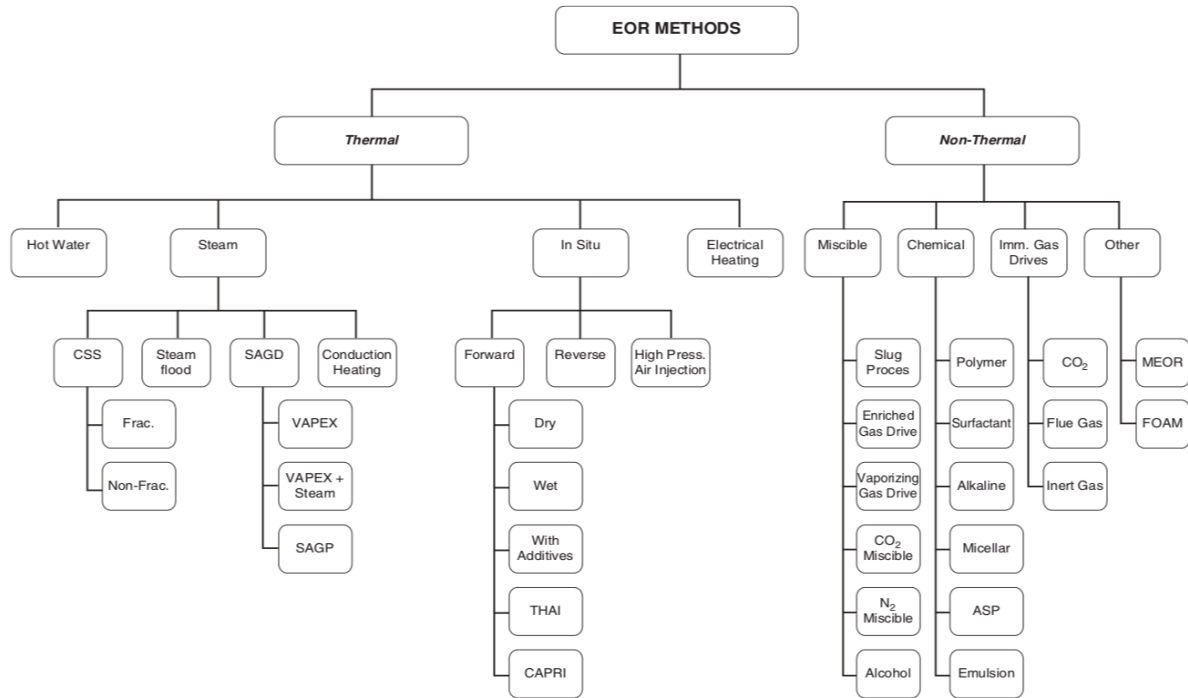
2.1 General Introduction to EOR Methods

Fossil fuels, like oil and gas, provide about 80% of the world's energy consumes. Besides, this energy demand is likely to increase in the future. Hence, it is vital to manage the production of oil from existing fields for as long as possible. As a result, it will be crucial to apply enhanced oil recovery (EOR). More than $2 * 10^{12}$ barrels of conventional oil and $5 * 10^{12}$ barrels of heavy oil remain in oil and gas reservoirs, using just nature drive mechanisms such as gas expansion, aquifer (water drive), solution gas drive, etc. (Thomas, 2008). In the early phase of oil production, the natural drive mechanism within the reservoir will be the method of choice to produce from the oil and gas. A common progression when the natural drive mechanisms lose their productivity is to consider water and gas injection through reservoir intervals. EOR is describe as every method that can be utilized to enhance oil recovery within a reservoir that does exclude natural drive mechanisms and injection of water and gas (Stosur, 2003). Such methods include heat transfer into heavy oil reservoirs, chemical injection, or inject microbes into the reservoir.

Enhanced oil recovery techniques, their utilization, and their classifications are shown in **Figure 1**. Polymer flooding implemented when an ample volume of the polymer is added to the water and inject into a reservoir with the intention of EOR. Appending polymer to water will raise the viscosity of the injected fluid. Also, this not only makes the mobility ratio to decline, but oil displacement through the porous media will be more efficient (Lake, 2014). Polymer flooding principally applied in the reservoirs with specific situations where conventional water flooding has low performance, such as fractured reservoirs or a reservoir with high permeable layer (thief zone) in which channeling phenomena may occur during water flooding, polymer gel usually used in this condition to shut off layer with high permeability (Speight, 2016).

To have a prosperous implementation of polymer flooding, it is obliged to have a proper propagation of polymer in porous media. Furthermore, a suitable concentration of polymer and proper viscosity and appropriate mobility ratio can aid considerably in achieving victorious polymer flooding. However, polymer retention may affect dramatically in weaken the performance of polymer flooding. Polymer retention ordinarily formed because of adsorption of polymer on the surface on the rock, and mechanical entrapment of polymer due to small pore throats size, and besides hydraulic retention of the polymer because of the high flow rate of injected fluid (Al-Hajri, 2018).

In this Thesis, aspects of mechanical entrapment and adsorption of the polymer as a fundamental phenomenon that impact on polymer EOR performance investigated.



EOR technique	Working Principle	Outcome / Results	When to use	Recovery rate
Gas Injection	Injecting gas or nitrogen (immiscible)	Push out crude or thins it , reduce rock-oil surface tension	Follow-up to water injection development (WAG – Water Alternating Gas Injection)	35% (variable)
Thermal Injection	Heat is injected to the reservoir to reduce the viscosity of the oil	Oil becomes lighter and flows more easily	Heavy crude fields	Up to 70%
Chemical Injection	Different type of chemicals (Polymers, Surfactants and others)	<ul style="list-style-type: none"> Reduce interfacial tension Increase flooded water viscosity 	Follows waterflood to capture residual oil; Sandstone reservoir and less Limestone	up to 15% incremental
CO2 injection	Injecting Carbon Dioxide (CO2)	CO2 swells oil and reduces viscosity	Follows waterflood to capture residual oil (generally used in Limestone reservoir)	up to 15% incremental

Figure 1 : EOR methods, applications, and recovery rate (Daleel Prteoleum L.L.C.) (Thomas, 2008)

2.2 Polymer

Polymer defined as a long chain, includes complex connected monomers and heavy molecular weight, regularly more than 200 gr/mole (Clark, 1982). The sorts of polymers tend to depend on characters of monomers and length of the chain. Regularly polymers with a longer chain, have more molecular weight, and consequently more viscosity in the dissolved state, which means more profitability and favorable mobility ratio (Gopferich, 1996). Nonetheless, polymers with long-chain chiefly degraded more. Furthermore, they can plug the pore throats and reduce the effective permeability. Therefore, determining the proper size of the polymer is an imperative subject in polymer flooding (Skauge, 2018).

Polymer partitioned to synthetic and biopolymer. Biopolymers have more productivity in high salinity water, however synthetic polymer such as Polyacrylamides has more efficiency in low salinity water. Consequently, picking the type of proper polymer is a function of properties of the reservoir such as water salinity, temperature, oil viscosity and so on (Needham, 1987). Plus, pore size distribution and heterogeneity of the reservoir are vital criteria that effect on polymer size.

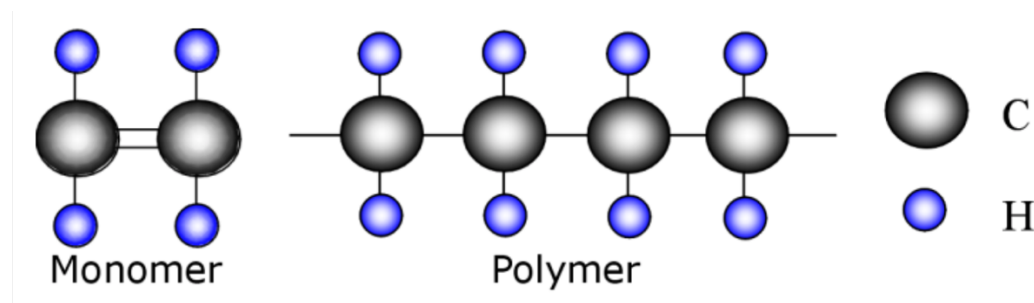


Figure 2 : Monomer and Polymer (usually polymer which used in EOR contains at least eight connected monomers chains) (UNSW, School of material science and engineering , 2013)

2.3 Polymer Flooding Mechanisms

Polymer flooding enhances oil recovery from 12% to 15% of oil in place (Hosseini, 2019). Viscous polymer solution flooded in the reservoir and lessens the mobility ratio between displacing fluid which is polymer dissolved water and displaced fluid which is oil. As a result, compared with traditional water flooding, the mobility ratio converts more favorable (Wei, 2014). Every

secondary and tertiary oil recovery method increases the recovery factor “RF”. Wherever the recovery factor is a function of volumetric sweep efficiency and displacement efficiency (Ahmed, 2012). Polymer does not affect residual oil saturation. Generally, the influence of polymer EOR is only represented in areal and vertical sweep efficiency. To minimize the residual oil saturation surfactant combined with the polymer and inject it into the reservoir. The surfactant diminishes the interfacial tension (IFT) and decreases the residual oil saturation (Karnanda, 2012). All in all, polymer added to water to increase the water viscosity, reduce the mobility ratio, and enhance sweep efficiency (Lake, 2014).

$$RF = E_{Vol}E_D = (E_A E_V)E_D \quad \text{Equation 1}$$

E_V = Vertical sweep efficiency
 E_D = Displacement sweep efficiency
 E_A = Areal sweep efficiency
 E_{Vol} = Volumetric sweep efficiency

2.3.1 Mobility Ratio

Mobility ratio determined as mobility of displacing fluid that can be water or polymer or foam or even gases such as CO₂, which are backward the shock front divided by the mobility of fluid-in-place which is oil or gas in hydrocarbon reserves and water in geothermal projects (Fanchi, 2002).

The main objective of polymer flooding is improving volumetric sweep efficiency by decreasing mobility ratios compare with traditional water flooding. Mobility ratio defined as a ratio of the displacing fluid (polymer) mobility to the displaced (oil) fluid in polymer EOR.

$$M = \frac{\lambda_{displacing\ fluid(water)}}{\lambda_{displaced\ fluid(oil)}} = \frac{k_{rw} \mu_o}{k_{ro} \mu_w} \quad \text{Equation 2}$$

The desirable mobility ratio is recognized as one or below one, where we do not have instability in the shock front and there is no viscose fingering. The mobility ratio, below one, indicated that

the displacing fluid, which is water/polymer, cannot transfer faster than displaced fluid (Ahmed, 2012). Yet, it is not regularly possible to have a mobility ratio below one, particularly in an extra-heavy oil reservoir, because of both economic issues associated with the expense of polymer and mechanical consideration of injection pressure (Lake, 2014). Injection pressure cannot exceed a specified value that identified as an operational limitation (Speight, 2016).

According to Equation 2 in order to decrease the mobility ratio and make mobility ratio more favorable we can :

- Decreasing the effective water permeability
- Increasing the effective oil permeability
- Decreasing the oil viscosity
- Increasing the water viscosity

Exchanging characteristics of the displaced fluid implemented by applying thermal recovery techniques nor polymer EOR. However, polymer flooding principally increases water viscosity and decreases effective water permeability (Ahmed, 2012).

By raising water viscosity and decreasing water effective permeability, the mobility ratio drops.

Mobility Ratio Calculation

Figure 3 represents the two shocks while polymer flooding. In the case of polymer EOR, two shock fronts befall (Pope, 1980). The initial saturation shock transpires between initial fluid-in-place and the displaced water and the second saturation shock among displaced water and the polymer solution.

Using linear stability analysis (Chorin, 1983) assisted to determine the mobility ratio where Sw_{f2} refers to the upstream front saturation at polymer-solution, Sw_{f1} assigned to water saturation at the oil bank and initial water saturation refers to Sw_{init} . The dashed line described polymer concentration.

$$M = \frac{(\lambda_w + \lambda_o)^{upstream}}{(\lambda_w + \lambda_o)^{downstream}} \quad \text{Equation 3}$$

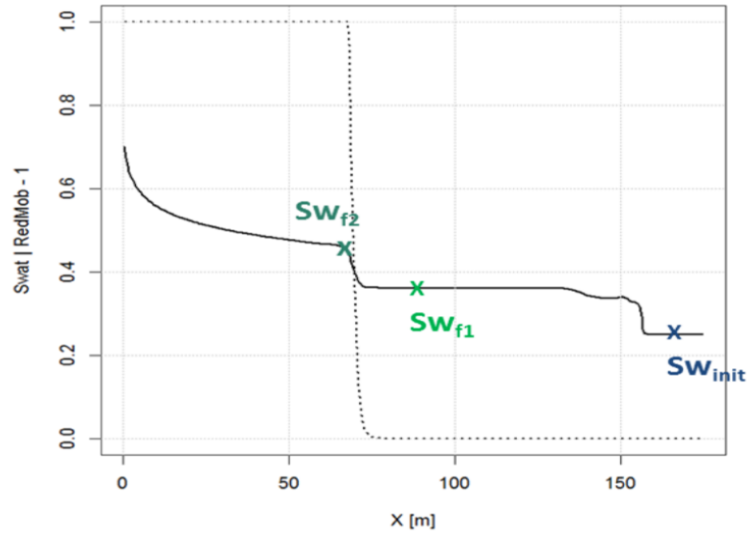


Figure 3: Water saturation profile during polymer flooding. Two saturation shock fronts will represent during polymer EOR, the first front represents the boundary between fluid-in-place and water. While the second front represents the boundary between polymer and oil-bank. The dash line shows the polymer concentration. After the second shock we do not have any chemicals. (Bouquet, 2017)

Figure 4 portrays the fractional flow function versus water saturation, where "J" is an injection point and "I" represents the primary condition in the reservoir before implementing EOR.

By drawing the tangent line from origin (0,0) to the polymer/oil line, we achieve point "A" (in the red line) and point "B" (in the blue line). The inclination of the line which connected origin to point A describes the speed of the polymer front ($V_{polymer\ front}$).

The intersection between the line crossed from the origin and the blue (water/oil) line expresses point "B", and the slope of a line that joined "B" to "I" (initial condition), represents the velocity of the oil-bank front ($V_{oil-bank}$).

The stability of the oil-bank front, the first front, chiefly depends on reservoir initial condition, such as primary oil and water saturation and reservoir heterogeneity and by injecting polymer we cannot make it stable. At the same time, the polymer can only impact on second saturation shock front stability. To guarantee we have stable polymer flooding the polymer front mobility consider less than the oil-bank front (W.B.Gogarty, 1970).

This implies that the mobility ratio at the second shock front obligation considers desirable (one or below one).

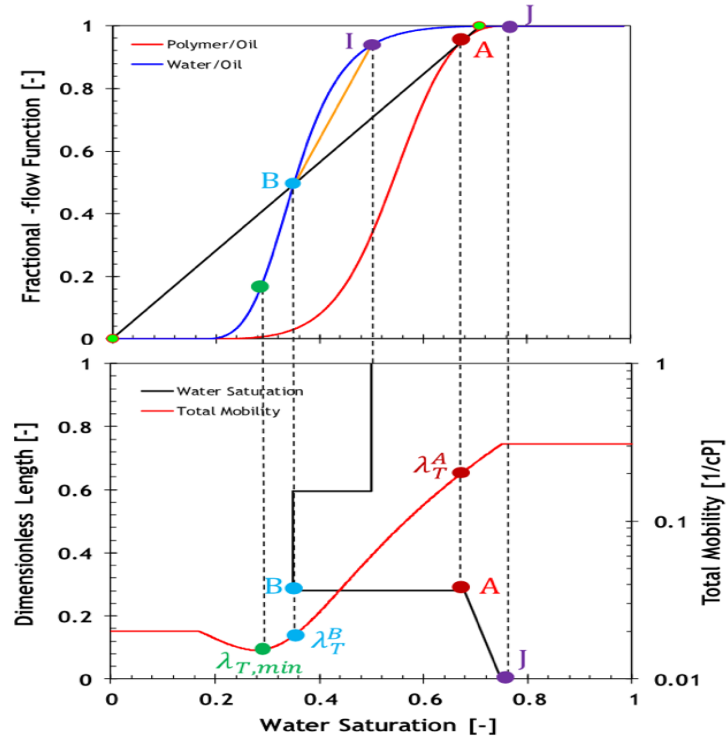


Figure 4 : fractional flow and dimensionless length vs. water saturation, the first and second shock front velocity can achieve using the following method. Point “J” represents the injection situation and point “I” displays the initial condition. (Farajzadeh, 2019)

Mobility ratio calculation with adsorption

To calculate the mobility ratio with acknowledging the adsorption, first of all, we have to define the retardation factor (D_s) which expresses the suspension in polymer saturation shock front due to adsorption (Moreno, 2016).

$$D_s = \frac{1 - \varphi \rho_s \Gamma_s}{\varphi \rho_w c_{inj}} \quad \text{Equation 4}$$

ρ_s : grain density

ρ_w : polymer solution density

Γ_s : adsorbed polymer on rock ($\frac{\mu g}{gr \text{ rock}}$)

c_{inj} : injected concentration of polymer in ppm

Accordingly, after calculating the retardation factor (D_S), we can apply the corresponding method. Nonetheless, instead of origin, we will draw the tangent line from $(-D_S, 0)$, as described in Figure 5a. Therefore, the position of points “A” and “B” will change and the velocity of the polymer front ($V_{polymer\ front}$) decreases.

As shown by Equation 4, the retardation factor depends on injection concentration, which implies that the adsorbed polymer will increase by higher polymer injected concentration (Figure 6).

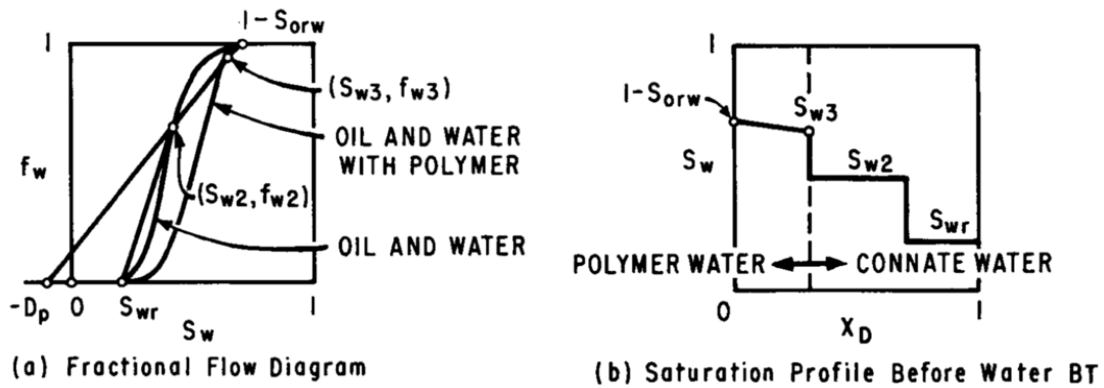


Figure 5: (a) Fractional flow diagram (with polymer adsorption), (b) saturation profile during polymer flooding (Pope, 1980)

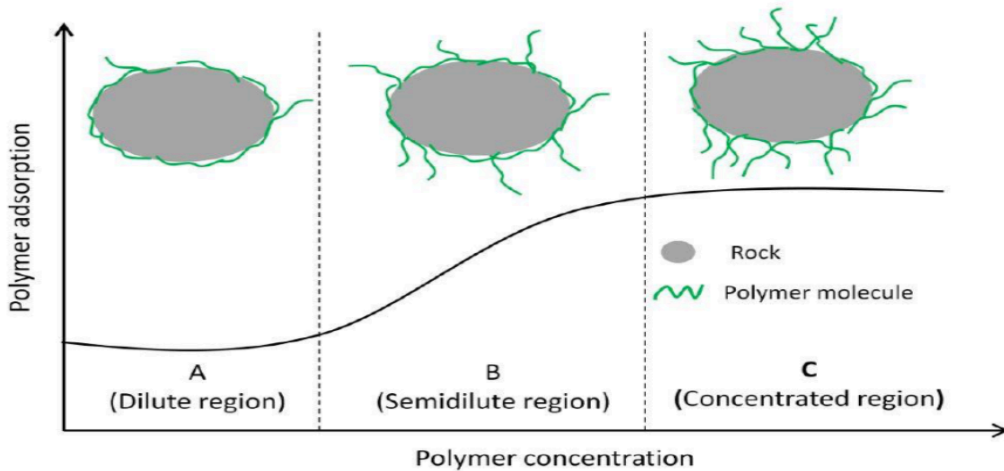


Figure 6: Polymer adsorption vs. polymer concentration. Ordinarily, by increasing the polymer concentration, the adsorption polymer will increase. (Zhang, 2014)

2.3.2 Sweep Efficacy

Polymer flooding influences on vertical and areal sweep efficiency, compared with conventional water flooding the mobility ratio will be decreases. Hence, the swept area will improvements.

Furthermore, in reservoirs with heterogeneity and anisotropy, polymer flooding can avoid channeling through the thief layer. . ($E_{volumetric} = E_{vertical}E_{areal}$) (Paul, 1982).

Vertical sweep efficiency is defined as the cross-section area contacted/total cross-section area. ($E_v = \frac{\text{cross section area contacted}}{\text{total cross section area}}$), Figure 7 represnts considerable effect of polymer flooding on vertical sweep efficiency, second layer obviously has high permeability, so the water flows faster in high permeable layer and the result could be low sweep efficiency and early breakthroughtime.

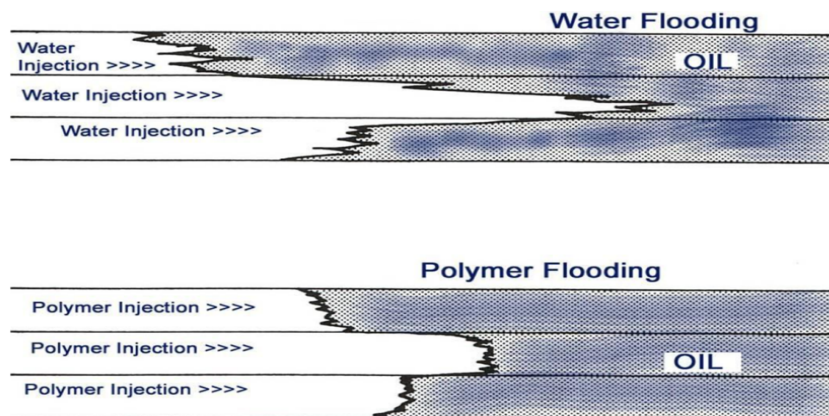


Figure 7: Vertical Sweep efficiency of water vs polymer flooding (Prasad, 2018)

Polymer flooding can increase the areal sweep efficiency which defined as, an area contacted/total area ratio. ($E_A = \frac{\text{area contacted}}{\text{total are}}$). Therefore, the most important role of polymer is increasing viscosity of injected fluid, which can improve sweep efficiency by decreasing mobility ratio.

The importance of polymer flooding effect can be most illustrate when we compare it with water-flooding, especially in case we have heterogeneous layers and cross flow between vertical layers.

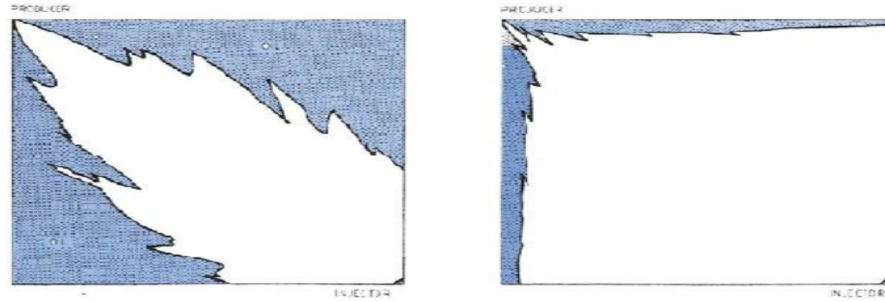


Figure 8: Areal sweep efficiency of water vs polymer flooding (Prasad, 2018)

The mobility effects significantly on sweep efficiency, according to Table 1 from “Advanced Reservoir Management and Engineering” book, areal sweep efficiency increases, by decreasing mobility ratio.

M	$1/M$	E_A at Breakthrough	E_A at 95% Water Cut
10	0.1	0.35	0.83
2	0.5	0.58	0.97
1	1	0.69	0.98
0.5	2	0.79	1.00
0.25	4	0.90	1.00

Table 1: Mobility ratio effect on areal sweep efficiency (Ahmed, 2012)

2.4 Polymer Retention

Polymer retention represents every mechanism responsible for diminishing the conventional velocity of polymer molecules when they transfer through the permeable reservoir. Polymer retention can be terminated by adsorption on the surface of the rock or mechanical plugging and trapping. The interaction between the rock surface and polymer molecules named adsorption. Adsorption determines polymer molecules bound to the surface of the rock thanks to electrostatic forces between the rock and polymer molecules (Zitha, 1998).

Polymer retention in a reservoir can appear because of polymer whether adsorption on a rock surface or mechanical entrapment inside pores and precipitation, due to the smaller size of pores throats compare to the size of polymer molecules. Mechanical entrapment commands the destruction of polymer stability. This implies a decline of polymer concentration in polymer

saturation shock and as a result, can damage mobility control. Polymer adsorption can compose a delay and retardation in the polymer front (Sorbie, 1991).

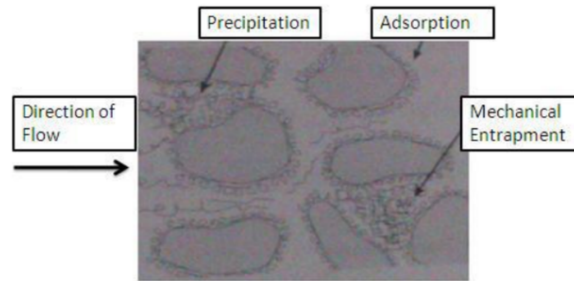


Figure 9 : polymer retention in porous media (Lake, 2014)

Mechanical entrapment or deep bed-filtration transpires when the polymer molecules pass through pores and ordinarily because of the small size of pore throats, they block the pores (Sorbie, 1991). The rate of polymer injection significantly depends on the maximum allowable pressure. However, as it represented Figure 10, the mechanical entrapment can raise the pressure in the injector. This implies polymers with larger size compared with the smallest pore throats, will capture and collapse the pore and consequently, we can observe permeability reduction and BHP increases.

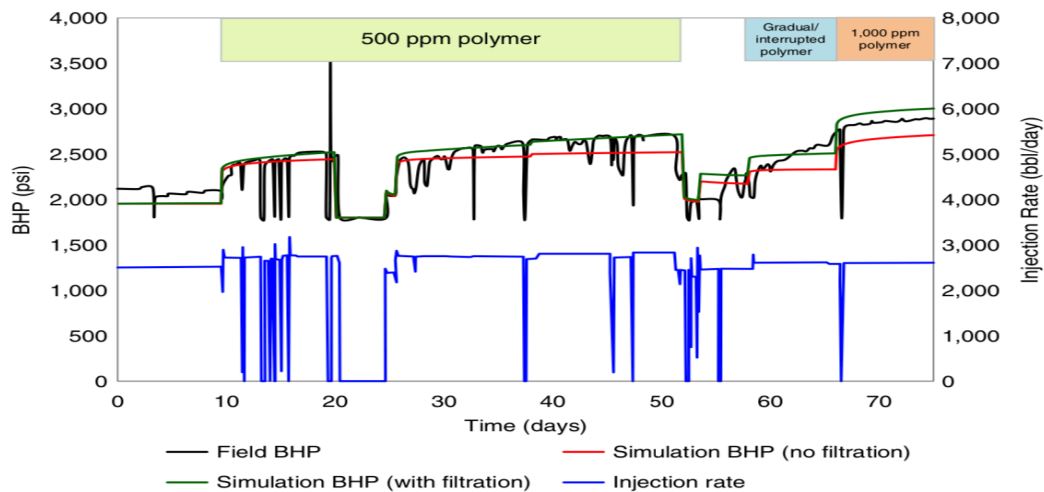


Figure 10 : field BHP and injection rate (Lotfollahi m. , 2015)

As depicted in **Figure 11**, polymers always have impurity, which determines that the size of all the molecules is not accurately equal, and seldom the largest size of polymers can block the pore throats. The principal consequence of polymer retention can consider as a permeability reduction. In Chapter 3, the equations related to polymer capture, and adsorption represented and in Chapter 4, we can see the influence of polymer retention on water saturation and mobility ratio of second saturation shock by numerical simulation.

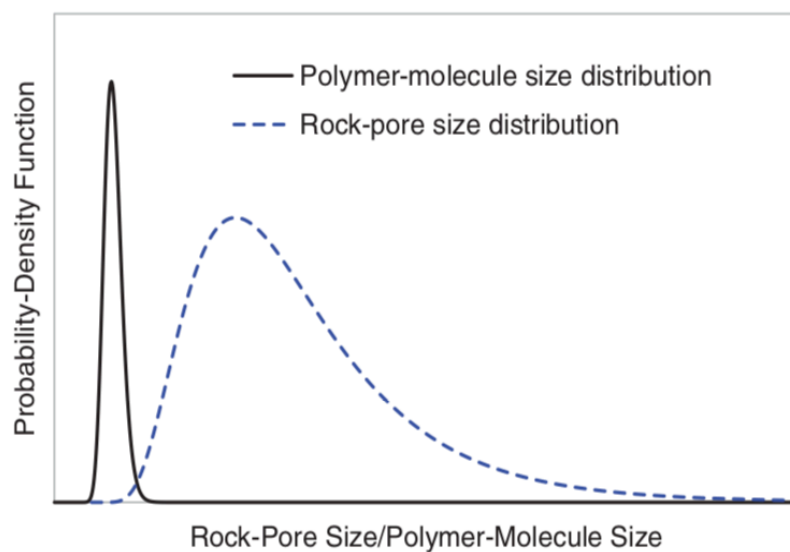


Figure 11: distribution of polymer molecule size and rock pore size (Lotfollahi M. , 2016)

Effective permeability reduction due to adsorption chiefly represented by the Langmuir equation and the permeability decline due to adsorption assumes irreversible and remains even after polymer flooding. Regularly, adsorption reaches the maximum amount after a reasonable long injection period. However, the concentration of polymer and pressure in the outlet constantly rises because of mechanical entrapment. (In case we did not consider back-pressure, constant pressure in the core's outlet.)

Chapter 3 *Physics and Mathematics*

3.1 Mass Conservation:

Total mass in the volume of “V”, by considering water density of “ ρ_w ”, the porosity “ φ ”, and water saturation equal to “ S_w ” is consider as “m”. Hence, the total mass can be obtained by computing total water mass in porous media multiply by water density. And the fraction of water volume in space is equal to “ φS_w ”. So, as a result, the total mass of water in the volume of “V” is equal to :

$$m = \iiint \rho_w \varphi S_w dV. \quad \text{Equation 5}$$

Mass rate, is total mass variation in volume of “V” with respect to the time, “t”. Therefore, by considering constant volume “V”, we can compute rate of mass variation by :

$$\frac{dm}{dt} = \iiint_V \left(\frac{d(\rho_w \varphi S_w)}{dt} \right) dV. \quad \text{Equation 6}$$

Mass flow can compute from Equation 7, where “s” is the surface area of the volume “V”, in which water transferred from. According to the Figure 12 “ u_{wn} ” is water velocity perpendicular to surface, “s” . Therefore mass flow can be obtain by equation below (where “ Φ ” is flux term):

$$\Phi = - \iint_S (\rho_w \underline{u_{wn}}) \cdot ds. \quad \text{Equation 7}$$

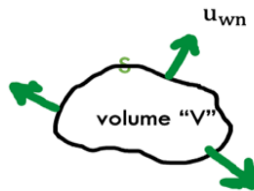


Figure 12 : mass exchange in a defined section with Volume "V".

Because we assume that there is no participation or source term inside the volume “V” and fluid is incompressible so we can emphasize that Equation 6 = Equation 7 :

Mass rate (kg/s)= Mass flow or flux (kg/s)

$$\iiint \left(\frac{d(\rho_w \varphi S_w)}{dt} \right) dV = - \iint (\rho_w \underline{u_{wn}}) \cdot ds. \quad \text{Equation 8}$$

So, in order to simplify the equation above, first of all, we can use the divergence theorem in the right hand side:

$$\iiint \left(\frac{d(\rho_w \varphi S_w)}{dt} \right) dV = - \iiint \nabla \cdot (\rho_w \underline{u_w}) dV. \quad \text{Equation 9}$$

Therefore, we just transfer the right hand side to the left and we can obtain one volume integral :

$$\iiint \left(\frac{d(\rho_w \varphi S_w)}{dt} + \nabla \cdot (\rho_w \underline{u_w}) \right) dV = 0. \quad \text{Equation 10}$$

It is obvious that, in the Equation 10, integral should be zero for any volume we consider (this means that any small volume element in fluid is always supposed so large that still contains a large number of molecules), so it only happens when the following integral is zero, and that is a partial differential equation that expresses our conservation of mass in general form :

$$\frac{\partial(\rho_w \varphi S_w)}{\partial t} + \nabla \cdot (\rho_w \underline{u_w}) = 0. \quad \text{Equation 11}$$

By considering that porosity is constant we can obtain that : (often the porosity is constant, unless we have deformation in our rock, which is not our case here) :

$$\varphi \frac{\partial(\rho_w S_w)}{\partial t} + \nabla \cdot (\rho_w \underline{u}_w) = 0. \quad \text{Equation 12}$$

For constant water density we obtain that (tend to when we work with water and oil, in order to simplify our equations, we can neglect compressibility of fluid, and also we can assume that density of water remain constant, so we can take out both “ ρ_w ”, so we have equation below which is our partial differential equation, shows mass conservation in pore volume) :

$$\varphi \frac{\partial S_w}{\partial t} + \nabla \cdot \underline{u}_w = 0. \quad \text{Equation 13}$$

similarly the oil equation obtain by considering the oil saturation of “ S_o ”. (In this equations we assume that we have two phase flow geometry, no gas exist is our system, in another word $S_w + S_o = 1$.)

$$\varphi \frac{\partial S_o}{\partial t} + \nabla \cdot \underline{u}_o = 0. \quad \text{Equation 14}$$

Where trivially divergence of “ \underline{u}_o ” is equal to (in 2D) :

$$\nabla \cdot \underline{u}_o = \frac{\partial u_o^x}{\partial x} + \frac{\partial u_o^y}{\partial y} \quad \text{Equation 15}$$

Now we can write Darcy equations for both the water and the oil, then we have : (where $\lambda_w = \frac{k_w}{\mu_w}$ is water mobility and $\lambda_o = \frac{k_o}{\mu_o}$ is oil mobility.)

$$\underline{u}_w = -\lambda_w \nabla P_w. \quad \text{Equation 16}$$

$$\underline{u}_o = -\lambda_o \nabla P_o. \quad \text{Equation 17}$$

Capillary pressure defines as a pressure variation between the non-wetting fluid in the reservoir and wetting fluid and then can determine as the following equation:

$$P_c = P_{nonwet} - P_{wet}. \quad \text{Equation 18}$$

Then just to simplified we consider in our case we have water wet reservoir, then we can obtain :

$$P_c = P_o - P_w. \quad \text{Equation 19}$$

3.2 Partial Differential Equations

Using mass conservation equations for oil and for water , Equation 13 and Equation 14, and by considering just oil and water in porous media (so we do not have gas), and by summation of two mass conservation equations for oil and water, we can obtain the following equation, which emphasis that divergence of total velocity is zero :

$$\varphi \frac{\partial}{\partial t} (S_w + S_o) + \nabla \cdot (\underline{u}_w + \underline{u}_o) = 0. \quad \text{Equation 20}$$

Total velocity consider as a constant volume. As a consequence the divergence of total velocity is zero :

$$\nabla \cdot (\underline{u}_w + \underline{u}_o) = \nabla \cdot (\underline{u}_{total}) = 0. \quad \text{Equation 21}$$

$$\underline{u_{total}} = \underline{u_w} + \underline{u_o} \quad \text{Equation 22}$$

Now by using Darcy (Equation 16 and Equation 17) equations in water and oil we can obtain :

$$\underline{u_{total}} = -\lambda_w \nabla P_w - \lambda_o \nabla P_o. \quad \text{Equation 23}$$

By using capillary pressure definition, Equation 19, we can replace P_o by $P_c + P_w$, in Darcy equation and we obtain:

$$\underline{u_{total}} = -\lambda_w \nabla P_w - \lambda_o \nabla (P_c + P_w) = -\lambda_w \nabla P_w - \lambda_o \nabla P_c - \lambda_o \nabla P_w. \quad \text{Equation 24}$$

We just simplify right hand side and we obtain :

$$\underline{u_{total}} = -\left(1 + \frac{\lambda_o}{\lambda_w}\right) \lambda_w \nabla P_w - \lambda_o \nabla P_c. \quad \text{Equation 25}$$

Now by using definition of fractional flow function we have following equation. (By considering, gravitation term and capillary term do not play a role in our equation. So the fractional flow can be simplified to the following equation):

$$f_w(S_w) = \frac{\lambda_w}{\lambda_w + \lambda_o}. \quad \text{Equation 26}$$

Using fractional flow definition, by considering no gravity and capillary term in definition of fractional flow function can help us to obtain :

$$\underline{u}_{total} = -\frac{1}{f_w} \lambda_w \nabla P_w - \lambda_o \nabla P_c. \quad \text{Equation 27}$$

By using Darcy equation in water, Equation 16, we can obtain the following equation :

$$\underline{u}_{total} = \frac{1}{f_w} \underline{u}_w - \lambda_o \nabla P_c. \quad \text{Equation 28}$$

And then we just multiples both left and right hand slides by f_w :

$$f_w \underline{u}_{total} = \underline{u}_w - f_w \lambda_o \nabla P_c. \quad \text{Equation 29}$$

Therefore, we can easily obtain \underline{u}_w from following equation and then we will use definition of fraction flow, Equation 26, and calculate : (where $\nabla S_w = \begin{pmatrix} S_{w,x} \\ S_{w,y} \end{pmatrix}$).

$$\underline{u}_w = f_w \underline{u}_{total} + f_w \lambda_o \nabla P_c = f_w \underline{u}_{total} - \left(-\frac{\lambda_o \lambda_w}{\lambda_w + \lambda_o} \right) \nabla P_c. \quad \text{Equation 30}$$

Therefore, Equation 31, represents the relation between water velocity, capillary pressure, and water saturation.

$$\underline{u}_w = f_w \underline{u}_{total} - \left(-\frac{\lambda_o \lambda_w}{\lambda_w + \lambda_o} \frac{dP_c}{dS_w} \right) \nabla S_w. \quad \text{Equation 31}$$

Then by definition, capillary diffusion coefficient can define using following equation:

$$-\frac{\lambda_o \lambda_w}{\lambda_w + \lambda_o} \frac{\partial P_c}{\partial S_w} = \hat{D}. \quad \text{Equation 32}$$

Therefore, we can easily obtain the equation for water velocity : (in order to simplify the equations we consider that, although \widehat{D} was function of S_w but we consider that D_{cap} is the same definition as \widehat{D} but is not anymore depends on S_w .)

$$\underline{u}_w = f_w \underline{u}_{total} - D_{cap} \nabla S_w. \quad \text{Equation 33}$$

Similarly we can obtain the oil by using Equation 22:

$$\underline{u}_o = f_o \underline{u}_{total} - D_{cap} \nabla S_o. \quad \text{Equation 34}$$

Now by using mass conservation equation, Equation 13, in water and replacing water velocity with the Equation 33, we can obtain : (by considering divergence of total velocity is equal to zero.)

$$\varphi \frac{\partial S_w}{\partial t} + \underline{u}_{total} \nabla f_w = \nabla \cdot (D_{cap} \nabla S_w). \quad \text{Equation 35}$$

Therefore, in 1D and two phase, it is dimensional partial differential equation which we have for saturation :

$$\varphi \frac{\partial S_w}{\partial t} + u_{total} \frac{\partial f_w}{\partial x} = \frac{\partial}{\partial x} D_{cap} \frac{\partial S_w}{\partial x}. \quad \text{Equation 36}$$

Now in order to make it dimensionless we can using following definition for dimensionless time, distance, and velocity, moreover we have equation for reference time :

$$\begin{aligned} t_R &= \varphi \frac{x_R}{u_R} & t_D &= \frac{t}{t_R} & x_D &= \frac{x}{x_R} \\ u_D &= \frac{u}{\frac{x_R}{t_R}} & P_R &= -\frac{\mu_w u_R x_R}{k} & P_D &= \frac{P}{P_R} \end{aligned}$$

Where t_R defined as a required time for the fluid to go through porous media with reference velocity (1PV). And P_R is defined as a pressure differences between inlet and outlet, to have a flow with contact velocity of u_R . By using dimensionless definitions and partial differential equation (PDE) which we have for saturation, Equation 36, we can obtain :

$$\varphi \frac{\partial S_w}{\partial(t_R t_D)} + u_{total} \frac{\partial f_w}{\partial(x_R x_D)} = \frac{\partial}{\partial(x_R x_D)} D_{cap} \frac{\partial S_w}{\partial(x_R x_D)}. \quad \text{Equation 37}$$

By divided both right and left hand sides to $\frac{u_{total}}{x_R}$ we can obtain the equation below:

$$\frac{x_R}{u_{total} t_R} \frac{\partial S_w}{\partial t_D} + \frac{\partial f_w}{\partial x_D} = \frac{x_R}{u_R} \frac{D_{cap}}{x_R^2} \frac{\partial^2 S_w}{\partial x_D^2}. \quad \text{Equation 38}$$

Therefore by definition of Peclet number (where $Pe = \frac{u_R x_R}{D_{cap}}$), we can simplified equation

and then we have :

$$\frac{\partial S_w}{\partial t_D} + \frac{\partial f_w}{\partial x_D} = \frac{1}{Pe} \frac{\partial^2 S_w}{\partial x_D^2}. \quad \text{Equation 39}$$

Similarly in 2D we know that :

$$\nabla \cdot (f_w u_{total}) = \frac{\partial(f_w u_{total}^x)}{\partial x} + \frac{\partial(f_w u_{total}^y)}{\partial y} = u_{total}^x \frac{\partial f_w}{\partial x} + f_w \frac{\partial u_{total}^x}{\partial x} + u_{total}^y \frac{\partial f_w}{\partial y} + f_w \frac{\partial u_{total}^y}{\partial y}. \quad \text{Equation 40}$$

Or in the other words we can implies that :

$$\nabla \cdot (f_w u_{total}) = \left(\frac{\partial f_w}{\partial x} \right) \cdot \left(u_{total}^x \right) + \left(\frac{\partial f_w}{\partial y} \right) \cdot \left(u_{total}^y \right) = \nabla f_w \cdot u_{total}. \quad \text{Equation 41}$$

As a consequence, the final equation for saturation in 2D is following equation, using Equation 31 :

$$\varphi \frac{\partial S_w}{\partial t} + (\nabla f_w) \cdot u_{total} = \frac{\partial(D_{cap} \frac{\partial S_w}{\partial x})}{\partial x} + \frac{\partial(D_{cap} \frac{\partial S_w}{\partial y})}{\partial y} = \nabla \cdot (D_{cap} \nabla S_w). \quad \text{Equation 42}$$

Therefore, the dimensionless form of the PDE equation of saturation can obtain as a : (where

$$u_D^x = \frac{u_{total}^x}{u_{injection}}, \text{ and } u_D^y = \frac{u_{total}^y}{u_{injection}}, x_D = \frac{x}{x_R}, y_D = \frac{y}{x_R}.$$

$$\frac{\partial S_w}{\partial t_D} + \left(\frac{\partial f_w}{\partial x_D} \right) \cdot \left(u_D^x \right) = \frac{1}{Pe} \left(\frac{\partial^2 S_w}{\partial x_D^2} + \frac{\partial^2 S_w}{\partial y_D^2} \right). \quad \text{Equation 43}$$

Therefore, we obtain the first equation related to saturation in 2D, assuming that there is incompressible fluid in porous media and by considering that capillary and gravitation is negligible. Now we need to obtain next equation for pressure. In order to obtain it first of all we need to use mass conservation equation, Equation 13 and Equation 14 and Darcy law Equation 23, which we already used to obtain previous partial differential equation.

We know that the divergence of total velocity is zero. Therefore, just by using Darcy law we can obtain following equation :

$$\nabla \cdot \underline{u_{total}} = \nabla \cdot (-\lambda_w \nabla P_w - \lambda_o \nabla P_o) = 0. \quad \text{Equation 44}$$

Using definition of capillary pressure can help us to simplified formula :

$$\nabla \cdot (-\lambda_w \nabla (P_o - P_c) - \lambda_o \nabla P_o) = 0. \quad \text{Equation 45}$$

$$\nabla \cdot (-(\lambda_w + \lambda_o) \nabla P_o + \lambda_w \nabla P_c) = 0. \quad \text{Equation 46}$$

$$\nabla \cdot (-\lambda_{total} \nabla P_o + \lambda_w \nabla P_c) = 0. \quad \text{Equation 47}$$

$$\nabla \cdot (\lambda_{total} \nabla P_o) = \nabla \cdot (-\lambda_w \nabla P_c). \quad \text{Equation 48}$$

By using definition of mobility we can obtain :

$$\nabla \cdot \left(\frac{kk_{rw}}{\mu_w} + \frac{kk_{ro}}{\mu_o} \right) \nabla P_o = \nabla \cdot \left(-\frac{kk_{rw}}{\mu_w} \nabla P_c \right). \quad \text{Equation 49}$$

Now, we use the dimensionless pressure definition to exchange the general equation to dimensionless form:

$$\frac{1}{x_R^2} \nabla_D \cdot \left(\frac{kk_{rw}}{\mu_w} + \frac{kk_{ro}}{\mu_o} \right) \nabla_D P_{o,D} P_R = \frac{1}{x_R^2} \nabla_D \cdot \left(\frac{kk_{rw}}{\mu_w} \nabla_D P_{c,D} P_R \right). \quad \text{Equation 50}$$

$$\frac{\mu_w}{kt_R} \nabla_D \cdot \left(\frac{kk_{rw}}{\mu_w} + \frac{k\mu_w}{\mu_w\mu_o} k_{ro} \right) \nabla_D P_{o,D} = \frac{1}{x_R^2} \nabla_D \cdot \left(\frac{kk_{rw}}{\mu_w} \nabla_D P_{c,D} P_R \right). \quad \text{Equation 51}$$

$$\frac{1}{t_R} \nabla_D \cdot \left(k_{rw} + \frac{\mu_w}{\mu_o} k_{ro} \right) \nabla_D P_{o,D} = \frac{1}{t_R} \nabla_D \cdot (k_{rw} \nabla_D P_{c,D}) \quad \text{Equation 52}$$

The equation below represents the partial differential equation for pressure in case we neglect effect of gravity. However we still consider capillary pressure on it :

$$\nabla_D \cdot \left(k_{rw} + \frac{\mu_w}{\mu_o} k_{ro} \right) \nabla_D P_{o,D} = \nabla_D \cdot (k_{rw} \nabla_D P_{c,D}) \quad \text{Equation 53}$$

We assume that the capillary pressure is negligible. Therefore, we can assume that $\nabla P_c = 0$.

And then by using the definition of total mobility we can obtain the following formula :

$$\nabla_D \cdot \left(k_{rw} + \frac{\mu_w}{\mu_o} k_{ro} \right) \nabla_D P_{o,D} = 0. \quad \text{Equation 54}$$

Similarly we can obtain the following partial differential equation for polymer concentration :

$$\varphi \frac{\partial(CS_w)}{\partial x_D} + \frac{\partial(Cu_w^x)}{\partial x_D} + \frac{\partial(Cu_w^y)}{\partial y_D} = \varphi D \frac{\partial(C \frac{\partial S_w}{\partial x_D})}{\partial x_D} \quad \text{Equation 55}$$

Where diffusion coefficient which we have in Equation 55, is molecular diffusion coefficient (D), while the diffusion coefficient in saturation partial differential equation, Equation 42, consider as a capillary diffusion. Therefore, in numerical simulation we have to consider this point in to our model.

3.3 Summary of Equations and Boundary Conditions

➤ Partial Differential Equation (PDE) for saturation considering no capillary and gravity forces:

$$\varphi \frac{\partial S_w}{\partial t} + \frac{\partial u_{wx}}{\partial x} + \frac{\partial u_{wy}}{\partial y} = \frac{\partial}{\partial x} \left(D_{cap} \frac{\partial S_w}{\partial x} \right) + \frac{\partial}{\partial y} \left(D_{cap} \frac{\partial S_w}{\partial y} \right).$$

$$\frac{\partial S_w}{\partial t_D} + \frac{\partial u_w}{\partial x_D} + \frac{\partial u_w}{\partial y_D} = \frac{1}{Pe} \left(\frac{\partial^2 S_w}{\partial x_D^2} + \frac{\partial^2 S_w}{\partial y_D^2} \right)$$

$$x_R = L$$

$$u_R = u_{injected} = \frac{-k P_R}{\mu x_R}$$

$$Pelet = \frac{u_R x_R}{D_{cap}}$$

$$t_D = \text{dimensionless time} = \frac{\varphi x_R}{u_R}$$

$$u_w^x = \text{water velocity in x direction} = \frac{-k k_{rw} \partial P}{\mu_w \partial x}$$

$$u_o^x = \text{oil velocity} = \frac{-k k_{ro} \partial P}{\mu_o \partial x}$$

$$u_w^y = \text{water velocity in y direction} = \frac{-k k_{rw} \partial P}{\mu_w \partial y}$$

$$P_R = \frac{-\mu_w u_R x_R}{k}$$

$$P_D = \frac{P}{P_R}$$

$$x_D = \frac{x}{x_R}$$

$$y_D = \frac{y}{x_R}$$

- Boundary Conditions used for saturation PDE :

Initial Condition (All domain) : S_{wc}

Source condition (Inlet) : $K \left(\frac{K_{rw}(1-S_{orw})}{\mu_p} \frac{\partial P}{\partial x} + \frac{K_{rw}(1-S_{orw})}{\mu_p} \frac{\partial P}{\partial y} \right)$

$$\text{Flux condition (Outlet)} : -K \left(\frac{K_{rw}(S_w)}{\mu_p} \frac{\partial P}{\partial x} + \frac{K_{rw}(S_w)}{\mu_p} \frac{\partial P}{\partial y} \right)$$

Zero Flux term : As it represents in **Figure 13**, we consider no flow from top and bottom of the defined model. This hypothesis applied in all 3 PDEs.

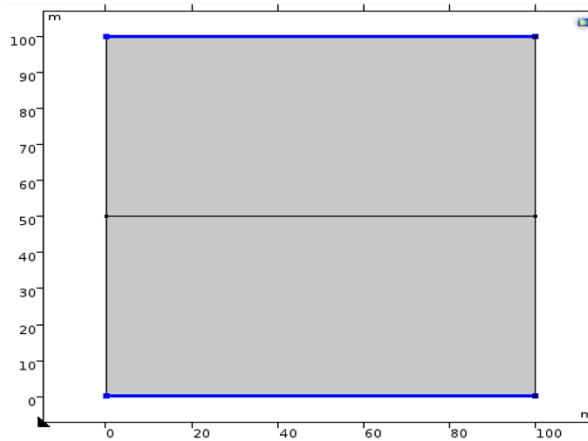


Figure 13: The blue lines in this figure shows the zero flux. Which means that we do not have any flow from these boundaries.

➤ PDE for Pressure : (Capillary pressure and gravity force are negligible)

$$\nabla \cdot \left(k \left(\frac{k_{rw}}{\mu_w} + \frac{k_{ro}}{\mu_o} \right) (\nabla P_D) \right) = 0$$

$$\left(k_{rw} + k_{ro} \frac{\mu_w}{\mu_o} \right) \nabla_D P_D = u_{total}$$

$$P_D = \frac{P}{P_R}$$

- Boundary Conditions used for pressure PDE :

Initial Condition (All domain): 20-10x

Dirichlet Boundary condition 1 (Inlet) : $10^6 Pa$

Dirichlet Boundary condition 2 (Outlet) : $10^4 Pa$

Zero flux term : exactly similar to **Figure 13**.

➤ PDE for Concentration : (Capillary pressure and gravity force are negligible)

$$\varphi \frac{\partial(CS_w)}{\partial x_D} + \partial_{x_D}(Cu_{wx}) + \partial_{y_D}(Cu_{wy}) = D\varphi \partial_{x_D}(C \partial_{x_D} S_w)$$

$$C_R = C_{injection}$$

D : molecular diffusion coefficient, which is different from diffusion term which we had in saturation PDE (that was capillary diffusion).

- Boundary Conditions used for concentration PDE :

Initial Condition (All domain) : 0

Dirichlet Boundary Condition (Inlet) : 1

Flux Condition (Outlet): C

3.4 Mechanical Entrapment and Adsorption

As we explained previously in Chapter 2, the polymer will improve the viscosity of the injected solution. The equation below expresses the relation between polymer concentration and injected viscosity. Where “m” and “n” obtain through experiments for which kind of polymer.

$$\mu_p = \mu_w(1 + mc + nc^2)$$

Equation 56

μ_p = polymer viscosity

n = viscosity coefficient

c = polymer concentration in aqueous phase m = viscosity coefficient

μ_w = water viscosity

Mechanical entrapment and adsorption principally effect on effective permeability. As it represented in the equation below, the adsorption and mechanical entrapment diminish permeability.

$$\frac{k(0,0)}{k(\hat{c}, \sigma)} = 1 + R\hat{c} + \beta\sigma \quad \text{Equation 57}$$

\hat{c} = adsorbed polymer concentration

R= permeability-reduction (or resistance) factor due to polymer adsorption

σ = trapped polymer concentration

β = formation damage coefficient

Tend to simulate polymer adsorption in porous media Langmuir equation used. The equation below represents the Langmuir equation in porous media.

$$\hat{c} = \frac{bC}{1 + bC} \widehat{C_{\max}} \quad \text{Equation 58}$$

$\hat{C} = \frac{\hat{c}}{\varphi c_0}$ dimensionless adsorbed polymer concentration

$\widehat{C_{\max}}$ = maximum dimensionless adsorbed – polymer concentration

b= Langmuir polymer adsorption parameter

φ = porosity

To compute the relative permeability, we utilized the Corey-type function which represented below.

$$k_{rw} = k_{rwe} S_{wn}^{n_w} \quad \text{Equation 59}$$

$$k_{ro} = k_{roe} (1 - S_{wn})^{n_o} \quad \text{Equation 60}$$

Where we have :

$$S_{wn} = \frac{S_w - S_{wc}}{1 - S_{orw} - S_{wc}} \quad S_w = \text{water saturation}$$

$$S_{wc} = \text{connate water saturation} \quad S_{orw} = \text{residual oil saturation}$$

$$k_{rw} = \text{water relative permeability} \quad k_{ro} = \text{oil relative permeability}$$

All in all, the pressure and concentration equations which we applied in 1D represented here. (In these formula we do not consider the diffusion coefficient)

$$\frac{\partial(CS_w + \hat{C}(C) + S)}{\partial t_D} + \frac{\partial(Cfw)}{\partial x_D} = 0 \quad \text{Equation 61}$$

$$\frac{\partial P}{\partial x} = \frac{u}{k_0} (\mu_w (1 + mc + nc^2) (1 + R\hat{c} + \beta\sigma)) \quad \text{Equation 62}$$

Where we have :

R = permeability reduction factor due to polymer adsorption

k_0 = total permeability

$x_D = \frac{x}{L}$ dimensionless distance

β = formation damage coefficient

$t_D = \frac{ut}{\varphi L}$ dimensionless time

u = aqueous phase Darcy velocity

$S = \frac{\sigma}{\varphi c_0}$ dimensionless trapped (retained) polymer concentration

\hat{c} = adsorbed polymer concentration

σ = trapped polymer concentration

Where in 2D the concentration PDE equation, will be as follow, Equation 63 :

$$\varphi \frac{\partial(CS_w + \hat{C}(C) + S)}{\partial x_D} + \partial_{x_D}(Cu_{wx}) + \partial_{y_D}(Cu_{wy}) = D\varphi \partial_{x_D}(C \partial_{x_D} S_w) \quad \text{Equation 63}$$

Chapter 4 *Numerical Simulation*

In this Chapter, we would like to determine the distinction between water flooding and polymer EOR and investigate the effect on mechanical entrapment and polymer adsorption on the efficiency of polymer flooding.

4.1 Water flooding

In this section, we considered that we have conventional water flooding in the reservoir with the following data.

L	Length	100[m]	μ_o	oil viscosity	90[cP]
K	Total permeability	100[mD]	n_w	$k_{rw} = k_{rwe} S_w^{n_w}$ Constant of Corey-type function	3
ϕ	Porosity	0.28	n_o	$k_{ro} = k_{row} (1 - S_{wn})^{n_o}$ Constant of Corey-type function	2
u	Total velocity	3.3e-6[m/s]	S_{wc}	Connate water saturation	0.2
μ_w	Water viscosity	0.65[cP]	S_{orw}	Residual oil saturation	0.25
k_{roe}	End point oil permeability	0.85	k_{rwe}	End point water permeability	0.25

Table 2 : data used for conventional water flooding in both heterogeneous and homogeneous reservoirs

This results are represented water flooding in homogeneous reservoir. Using data at Table 2.

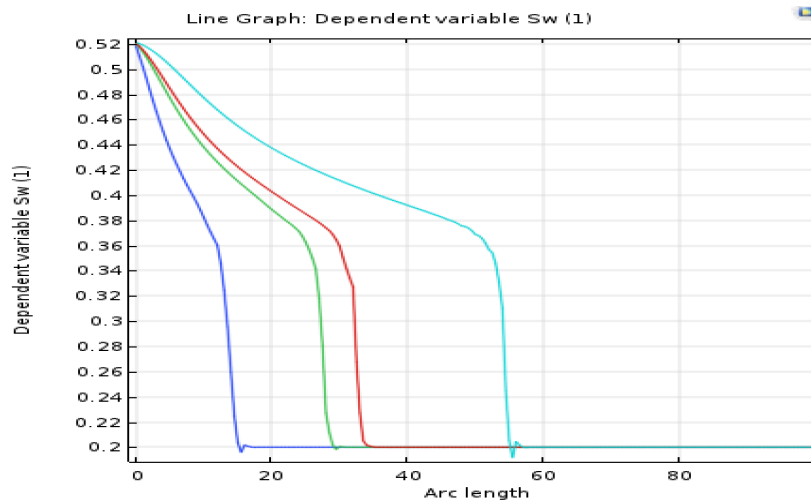


Figure 14: water saturation vs. length in homogeneous reservoir at 0.17 pore volume injected (PV), 0.28 PV, 0.32 PV and 0.55 PV which represent that water saturation at upstream shock is 0.37 and at the downstream is 0.2.

According to Equation 59 and Equation 60, we can calculate the relative permeability of oil and water using the data at Table 2. Therefore as it represents in Figure 15, the relative water and oil permeability as a function of water saturation represented. We use the following figure for all the models in this Chapter. The Figure 16, represents the water flooding in porous media with the data represented in Table 2. (Mobility ratio is more than 1 in this case, so it is unstable flow)

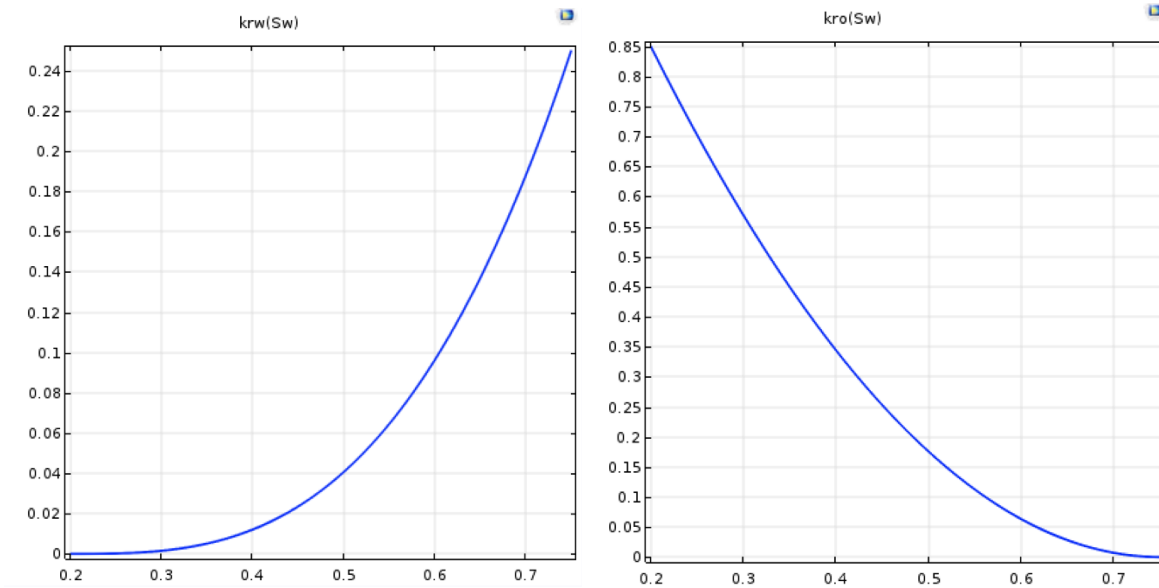
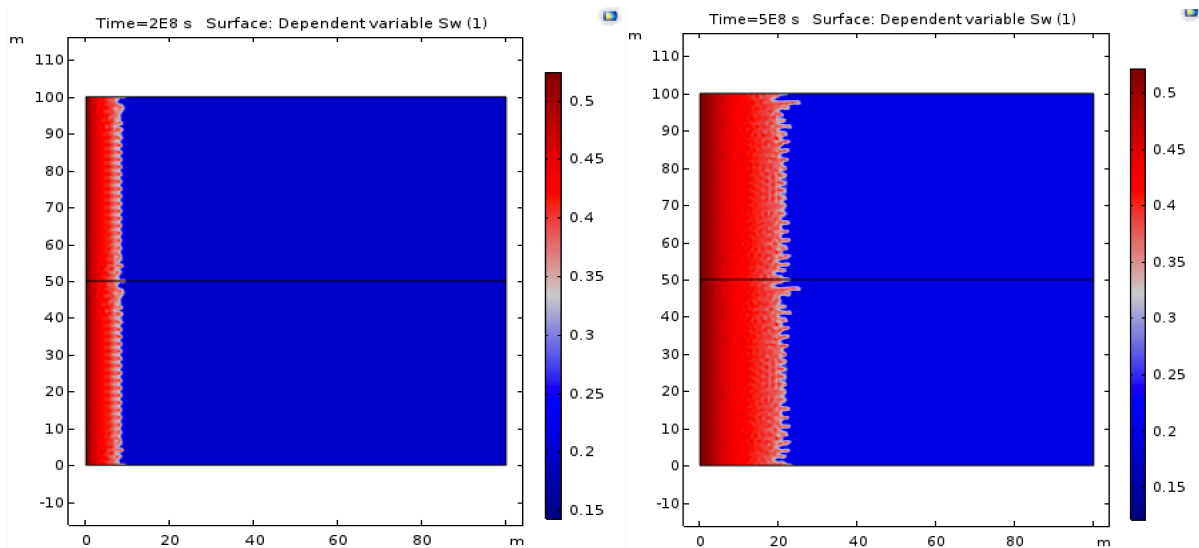


Figure 15: oil and water relative permeability vs. water saturation using Corey-type function



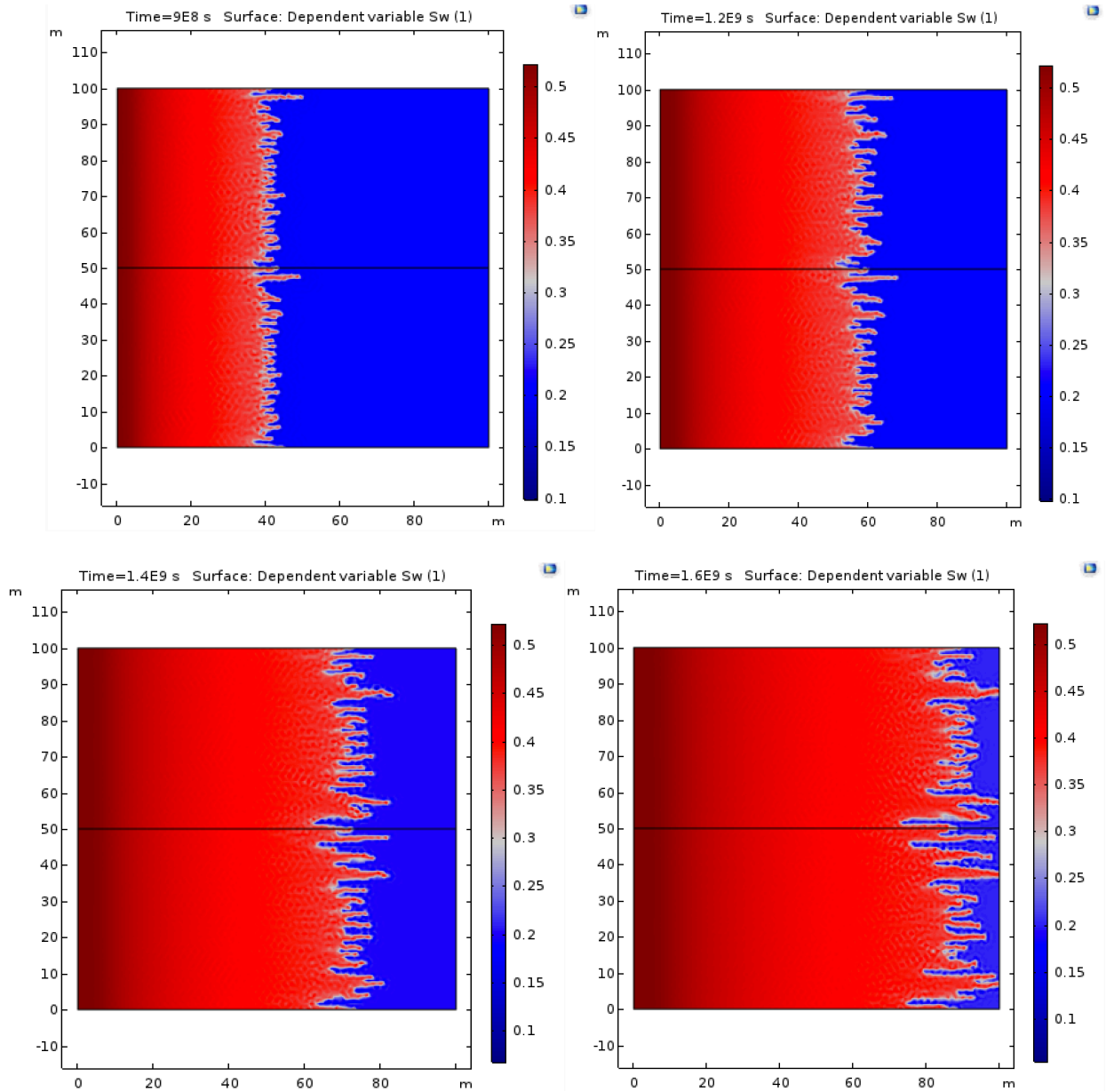


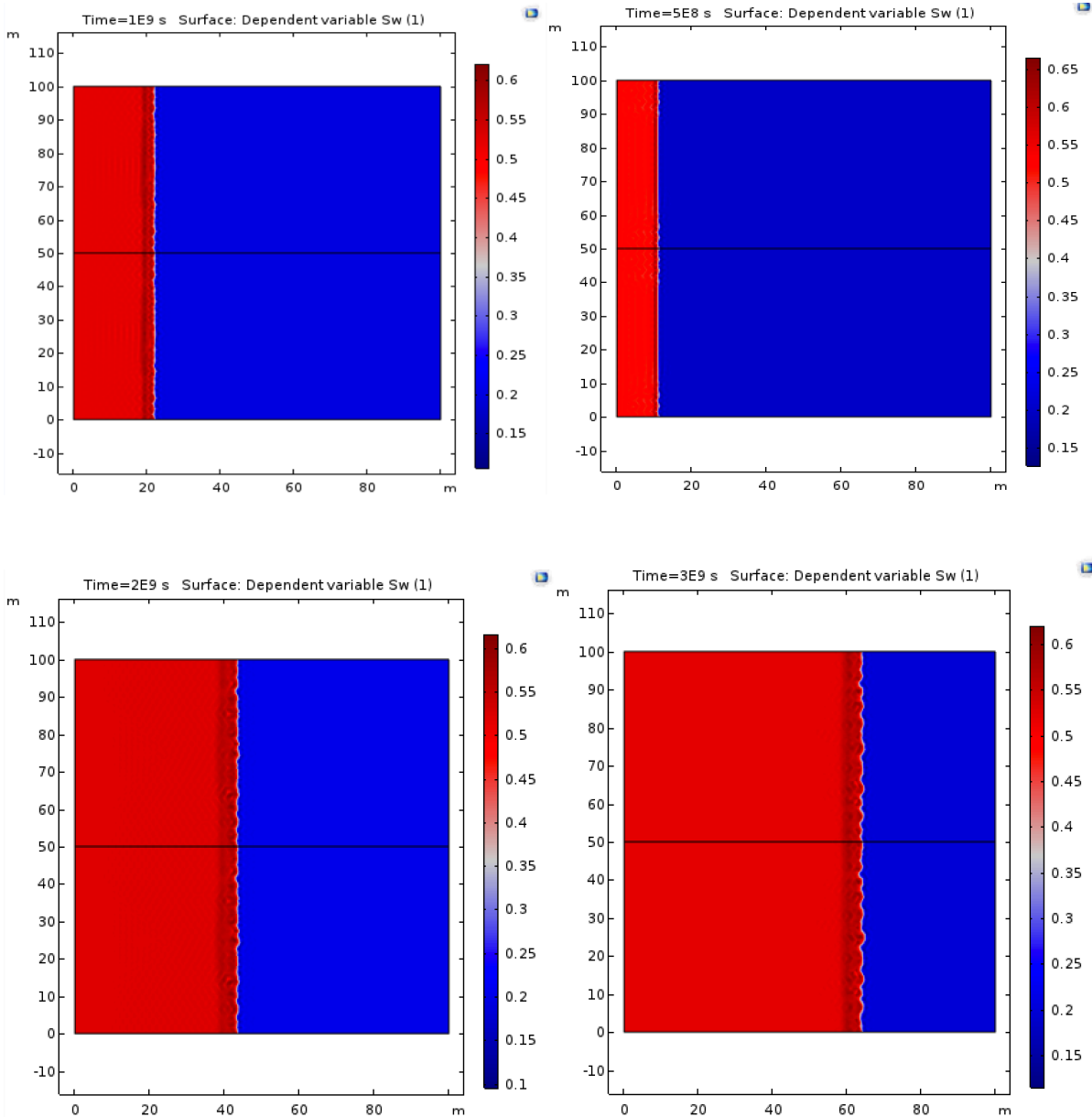
Figure 16: water flooding in reservoir and viscous fingering due to high mobility ratio (mobility ratio above 1)

$$\text{In this case mobility ratio can compute as } M = \frac{(\lambda_w + \lambda_o)_{upstream}}{(\lambda_w + \lambda_o)_{downstrwam}} = \frac{\left(\frac{k_{rw}(s_w(0.37))}{\mu_w} + \frac{k_{ro}(s_w(0.37))}{\mu_o} \right)}{\left(\frac{k_{rw}(s_w(0.2))}{\mu_w} + \frac{k_{ro}(s_w(0.2))}{\mu_o} \right)} =$$

1.7. Consequently, because the mobility ratio is unfavorable, we will have viscose fingering and instability in the shock front. Polymer combined to water in a diminutive volume to enhance water

viscosity and sweep efficiency. Polymer does not affect residual oil saturation and to decrease it, ordinarily, surfactant added to the polymer to diminish interfacial tension (IFT) and by modifying the wettability, mobility of both oil and water increased in the reservoir.

By changing the water parameter, we changed the mobility ratio to one to monitor stability in the water shock front.



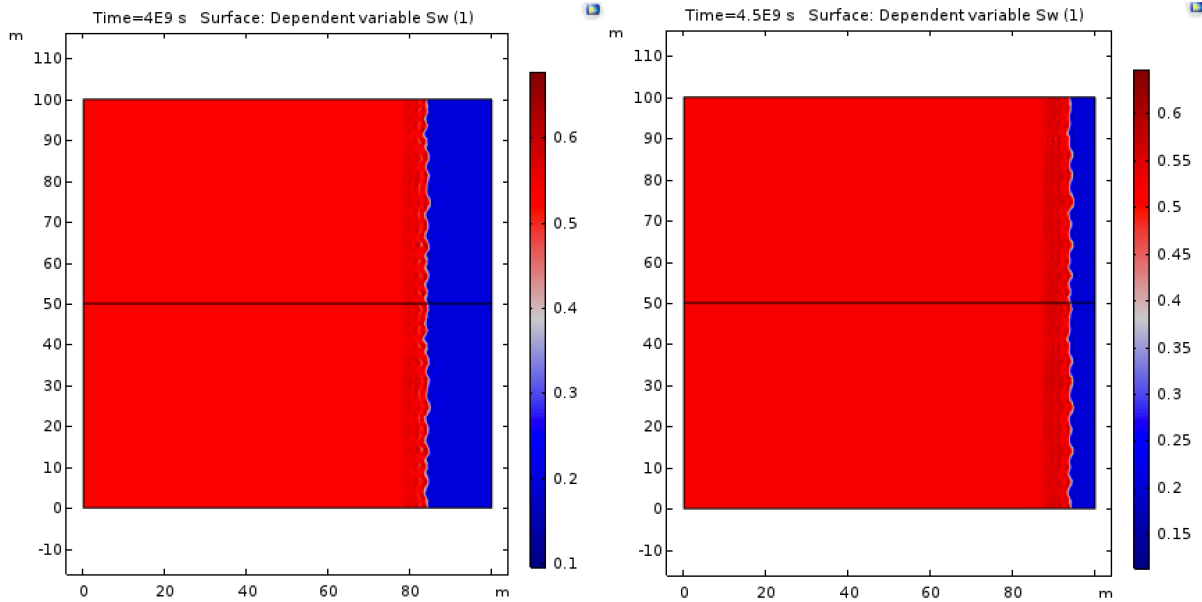


Figure 17: Water flooding with the favorable mobility ratio, so the viscose fingering disappeared and water shock front is stable.

4.2 Polymer flooding

The polymer increases the viscosity of displacing fluid and significantly improve areal and vertical sweep performance. In this segment, we first examine 1 Phase flow (merely water) and observe the influence of polymer entrapment and adsorption in 1D.

4.2.1 Single phase flow

In this segment, first of all, we acknowledge, we have a fully saturated core with a length of 1m (without any oil) and then we begin to inject the polymer. We would like to investigate the impression of adsorption and polymer entrapment in our model. Adsorption can be the purpose of retardation in the water saturation front. Consequently, as much as adsorption increments in our model, the polymer flows slower. Nonetheless, adsorption does not affect polymer concentration significantly, while mechanical entrapment principally effects of polymer concentration and influential effect on polymer saturation shock front retardation.

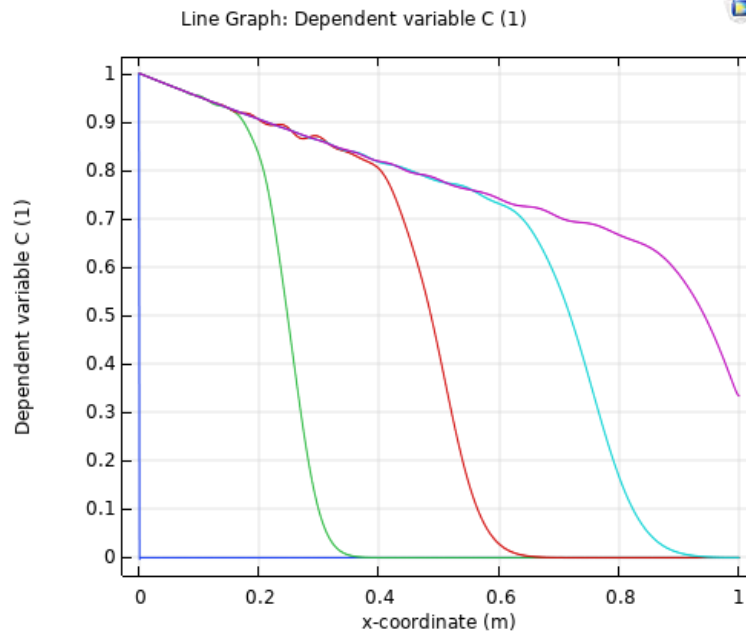


Figure 18 : the polymer concentration for a case we do not have adsorption. Mechanical entrapment decreases the polymer concentration at the saturation shock front

As it represented in Figure 18, in case the we do not have adsorption ($\hat{C}_{max} = 0$) and with considering constant filtration coefficient ($\Lambda = 0.5$), the polymer concentration decreases thanks to mechanical plugging. (where Λ define as a dimensionless filtration coefficient).

The definition of filtration coefficient represents in below :

$$\lambda(\sigma) = \lambda_0 \left(1 - \frac{\sigma}{\sigma_{max}}\right) \quad \text{Equation 64}$$

$\lambda_0 =$ filtration coefficient at zero polymer retention

$\sigma_{max} =$ maximum trapped (retained) polymer concentration

$$\frac{\partial S}{\partial t_D} = \Lambda C \quad \text{Equation 65}$$

$\Lambda = \lambda(\sigma)L$ dimensionless filtration coefficient

$$S = \frac{\sigma}{\varphi c_0} \text{ dimensionless trapped (retained) polymer concentration}$$

The retained polymer also is the function of time and consequently pore volume injected. By increasing PV the captured polymer concentration improved. In below the dimensionless retained polymer concentration in 0.25, 0.50, 0.75 and 1 PV expressed.

As it expected, by increasing injected pore volume the polymer retention increased. In Figure 19, the adsorption does not play a role which means that the maximum dimensionless adsorbed polymer concentration is zero (\hat{C}_{max}). The length of the domain consider as 1 meter and the filtration coefficient is constant. (dimensionless filtration coefficient is $\Lambda = 0.5$)

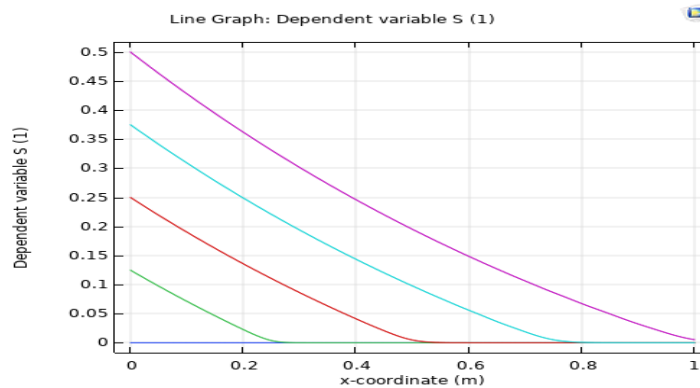


Figure 19: Dimensionless trapped polymer concentration in case we have constant filtration coefficient. (the polymer adsorption neglected in this figurer)

As much as filtration coefficient increase, the polymer concentration at the shock front decreases which means that displacing fluid viscosity will be decrease which leads to have instability in shock front. In Figure 20, the dimensionless filtration coefficient is 2, but in Figure 21, it is 0.5. As it represented in figures by increasing mechanical entrapment the concentration of polymer at the shock decreases and moreover retardation in polymer propagation happen (similar to polymer adsorption).

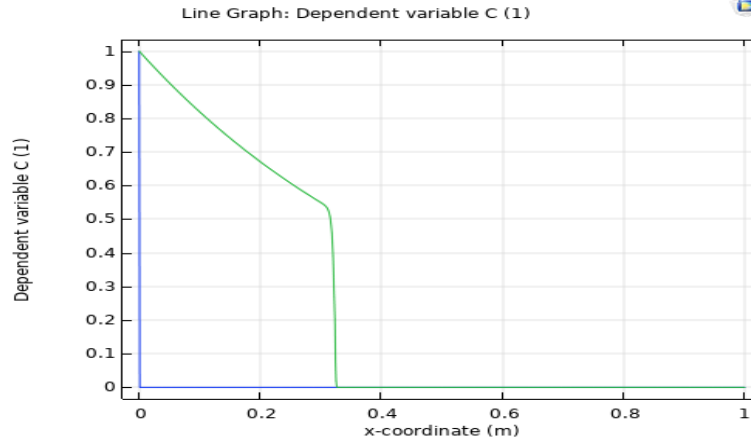


Figure 20 : Propagation of polymer in porous media is mainly rely on mechanical entrapment. In this figure $b=10$ (Langmuir polymer adsorption parameter), and maximum dimensionless adsorbed polymer concentration is 0.5 ($\hat{C}_{max} = 0.5$), and dimensionless filtration coefficient is 2 ($\Lambda = 2$).

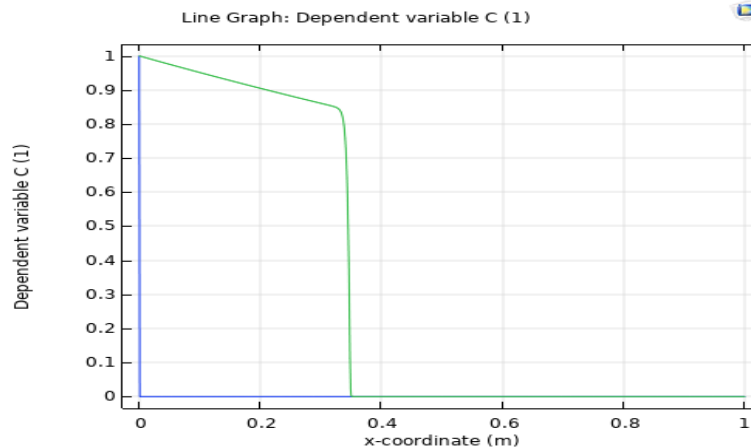


Figure 21: The adsorption data in exactly same as Figure 20. However in this case the dimensionless filtration coefficient decreases to 0.5 ($\Lambda = 0.5$).

In numerical modeling the diffusion coefficient play an important role in the model result. (As much as diffusion coefficient is smaller, the reliability of the model increases.). Figure 22, shows the outlet concentration data from experiment and matched simulation. Thanks to analytical solution the $\Lambda_0 = 0.438$ and $S_{max} = 0.695$ are fitted to the experimental data. (the filtration coefficient is not constant here.)

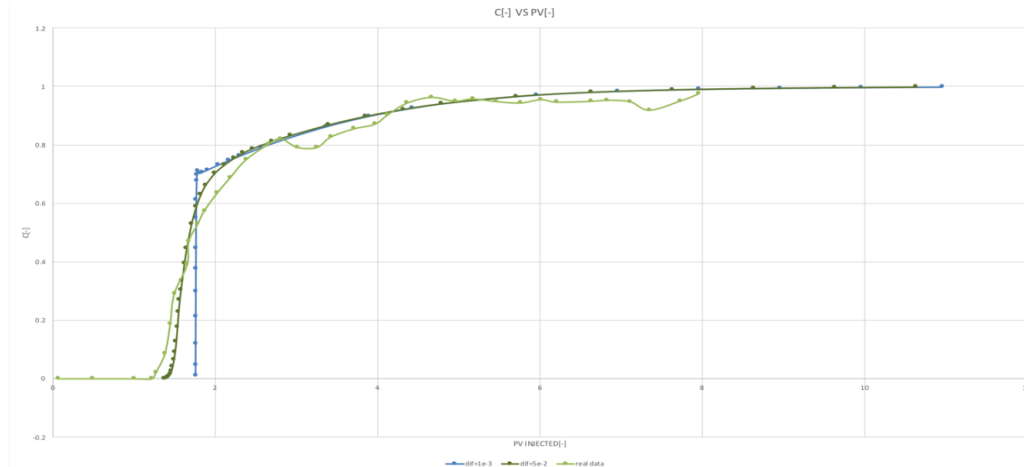


Figure 22: Outlet polymer concentration vs. pore volume injected. The diffusion coefficient effect represented in the figure (By decreasing diffusion coefficient dispersion of concentration increases and model has better match with experimental data. However analytical solution matched with blue line) .

4.2.2 Two phase flow

In this illustration, we have both oil and water in the porous media; next, we start to infuse the polymer in porous media. we will calculate the mobility ratio from the method which we beforehand described in Chapter 2. we analyze complex situations, with or without adsorption and mechanical entrapment to investigate specifically how these two phenomena will influence the mobility ratio and concentration variation. Furthermore, we modeled the water saturation structure in various statuses. Hence, we have sufficient knowledge to acknowledge, whereby adsorption and mechanical entrapment impacts the propagation of polymer in porous media.

Polymer Flooding, Without Mechanical Entrapment.

In this case we consider we do not have adsorption nor retention in porous media. The insert data is as follow. The insert data is represented in Table 2.

time t (s)	distance x(m)	Saturation (S_w)	k_{rw} (relative water permeability)	k_{ro} (relative oil permeability)	water viscosity [cP]	Oil viscosity [cP]	Mobility Ratio
0,05	0,071	0,535	0,0749	0,093	0,65	90	1,034158362
0,1	0,153	0,528	0,07138	0,0992	0,65	90	0,997234335
0,15	0,238	0,523	0,0689	0,10368	0,65	90	0,971343204
0,2	0,319	0,5235	0,0695	0,1032	0,65	90	0,978274278
0,25	0,401	0,5232	0,0695	0,103	0,65	90	0,97805334
0,3	0,483	0,523	0,0689	0,10368	0,65	90	0,971343204

Table 3: Insert data in the model with considering no mechanical entrapment and no adsorption in porous media. The polymer viscosity is 8 cP and the data of Table 2 used in this model

simply we can compute the mobility ratio utilizing figure 12 and figure 13. we have the concentration of polymer which is constant. In this example, we do not have any mechanical entrapment and adsorption. Furthermore, from a saturation figure, we can calculate the relative permeability of water and oil, applying the Corey type function. Accordingly, we can compute the mobility ratio. In this example, the mobility ratio is about 1, so we will have a stable saturation shock front. The mobility ratio is related to the chemical-oil-bank shock front.

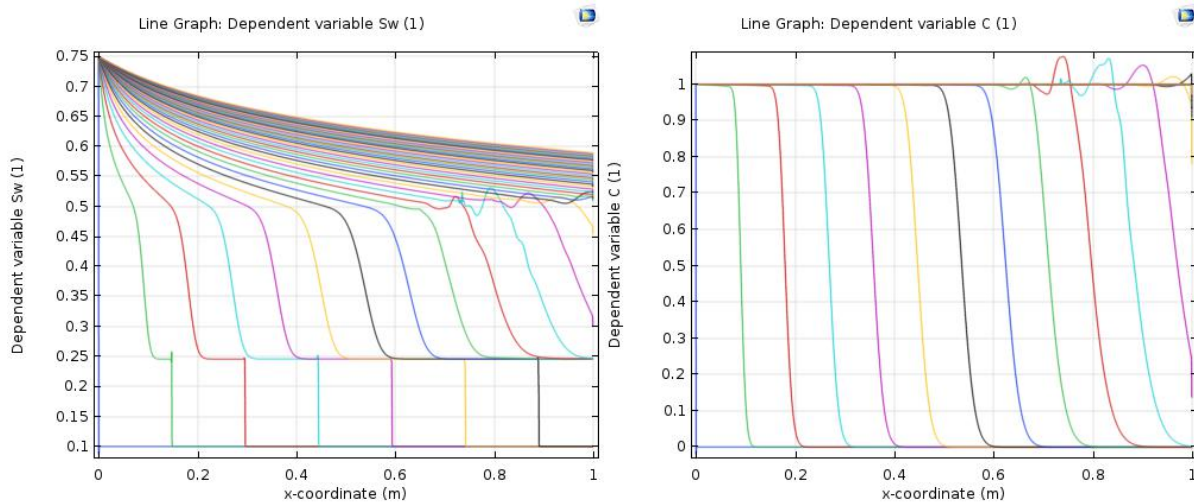


Figure 23: The polymer flooding, without adsorption and mechanical entrapment. The mobility ratio is about 1. and the polymer viscosity id 8 cP. Therefore, we do not have any viscous fingering or instability in this case. The instability represented in last time steps is due to low amount of diffusion coefficient, so it is numerical issue. Time steps here is 0.05 pore volume injected.

Presently in the next case, we examine that in the case in Equation 56, if we diminish the amount of the "m" and "n", the entire viscosity of the polymer solution will be diminished. This implies that in the system, we will have less stability compared with the former simulation. Accordingly, the mobility ratio will increase and rise above one. which indicates that the polymer solution transfers faster compared with the oil-bank. It is assumed that we will have instability or viscous fingering.

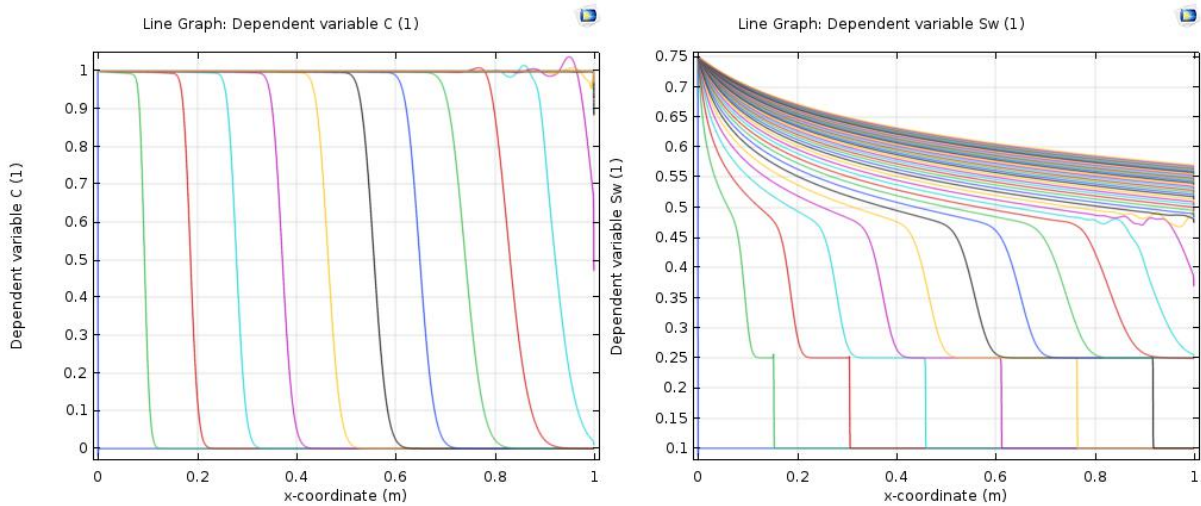


Figure 24: This figures represents the water saturation and the polymer concentration in the case that the polymer-solution viscosity id 6 cP. Therefore, compare with the previous case the water saturation at the oil-bank will decreases, the mobility ratio increases and the polymer concentration remains constant. Because in these two we do not have adsorption or mechanical entrapment of the polymer. Therefore the dimensionless polymer concentration is 1, and after polymer front it drop rapidly to zero.

time t (s)	distance x(m)	Saturation (Sw)	polymer viscosity (cP)	Krw (relative water permeability)	Kro (relative oil permeability)	Mobility Ratio
0,05	0,076	0,506	6,0329126	0,06093	0,1197	1,118861379
0,1	0,16	0,501	6,0329126	0,0587	0,1248	1,088224024
0,15	0,242	0,50178	6,037746936	0,0595	0,12395	1,099507463
0,2	0,326	0,50125	6,03895565	0,05882	0,12448	1,08886804
0,25	0,411	0,5012	6,040164416	0,05882	0,12448	1,08867723
0,3	0,496	0,5002	6,040164416	0,0584	0,12555	1,083034207

Table 4: In the polymer viscosity 6cP and time step 0.05 Pore Volume Injected (PV)

The most crucial feature that has to take into account is water saturation in the case of the polymer viscosity shift from 8 cP to 6 cP. The water saturation varieties from 0.523 to 0.50 at the polymer saturation shock front.

similarly, in case we increase the water viscosity which implies that by supplementing polymer to the polymer-solution, enhance the concentration of polymer and consequently improve its viscosity, the mobility ratio will decline to 0.75, which indicates more stability and no viscous fingering.

Polymer Flooding, with Mechanical Entrapment

In the subsequent step, we modeled the polymer flooding by examining the mechanical entrapment phenomena. As we explained previously, the polymers may have sizes more than the smallest pore throats, Figure 11. Accordingly, some polymers trapped the pores and decrease the effective permeability and furthermore diminish the concentration of the polymer at the polymer solution saturation shock front.

Hence, a lower concentration is the principal motivation for decreasing viscosity in polymer solution saturation shock front and more mobility ratio. In former we calculate that in case the polymer viscosity is 8 cP and utilizing the data in Table 2, the mobility ratio is 1, desirable. (Table 3 and Figure 23). Presently, we assume that in case we have mechanical entrapment what would occur to the mobility ratio and polymer concentration.

λ_0	Filtration coefficient at zero polymer retention	$0.438 \frac{1}{m}$
β	Formation damage coefficient	2000
Diffusion	Diffusion coefficient in 1D	10^{-5}
σ_{max}	Maximum trapped polymer concentration	0.696

Table 5: these data used for model the mechanical entrapment in porous media. We do not consider adsorption in this simulation.

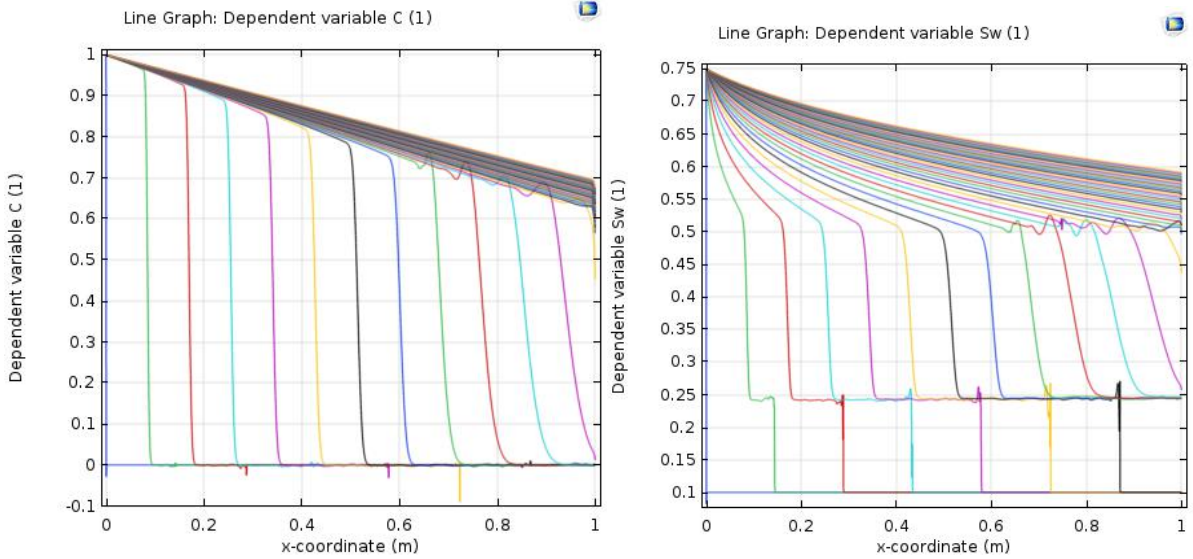


Figure 25: Polymer flooding in case we have mechanical entrapment in porous media. Therefore, the concentration of the polymer as it represented in the figure will drop, as a function of pore volume injected or time. As a result, the mobility ratio will increase. In this case we used $\lambda_0 = 0.438 \frac{1}{m}$.

time t (s)	distance x(m)	Saturation (Sw)	Dimensionless Concentration	polymer viscosity (cP)	Krw (relative water permeability)	Kro (relative oil permeability)	Mobility Ratio
0,05	0,076	0,5225	0,964	7,7080224	0,0687	0,1042	1,023538568
0,1	0,1556	0,5192	0,927	7,41482885	0,06705	0,1072	1,040128871
0,15	0,241	0,5112	0,888	7,1077136	0,0637	0,1148	1,040520033
0,2	0,325	0,5064	0,852	6,8259776	0,0611	0,1194	1,044597242
0,25	0,41	0,502	0,816	6,5459264	0,0591	0,1237	1,057321615
0,3	0,492	0,501	0,785	6,30612125	0,0587	0,1247	1,086899018

Table 6: The mobility increases and it is function of PV. In case we do not have polymer retention the mobility at the same condition is below one. However, in this case the mobility ratio raised up and we have instable situation. The “m” and “n” which is used in this model (according to Equation 56) are 10.3 and 1.

As represented in Figure 25, the concentration of polymer decreases when we examine mechanical entrapment in porous media. Accordingly, in case we have a mechanical entrapment, the mobility ratio arises and we will have instability. Comparison between Table 6 and Table 3, explicates how mechanical entrapment can affect polymer flooding efficiency. Therefore, to

compensate for the impact of mechanical entrapment we have to increase the concentration of polymer in porous media. it implies that more polymer must be used to have a desirable mobility ratio.

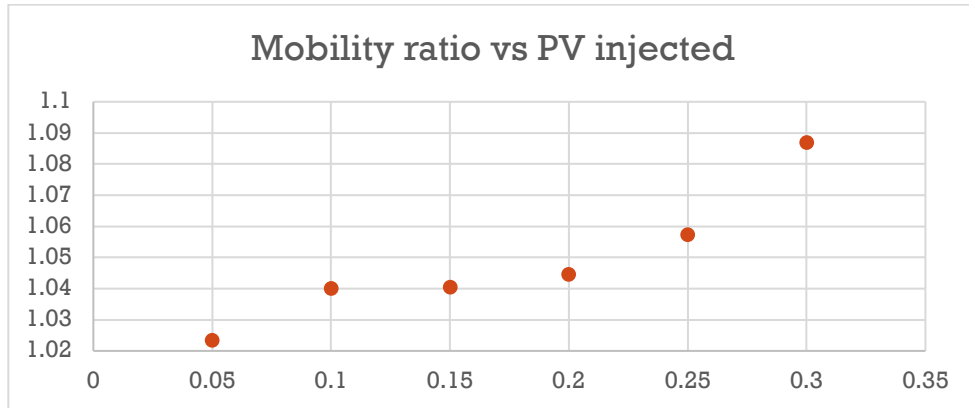


Figure 26: In case we have mechanical entrapment, the mobility ratio increased by time (PV injected) which means that the concentration of polymer decreases constantly and reduction of polymer concentration leads to have more mobility ratio.

In the following example, we examine that in case we increase "m" in equation 56 from 10.3 to 20, and consequently change the polymer viscosity, the mobility ratio drops. However, still by increasing pre volume injected, the mobility ratio rises and the polymer concentration reduced.

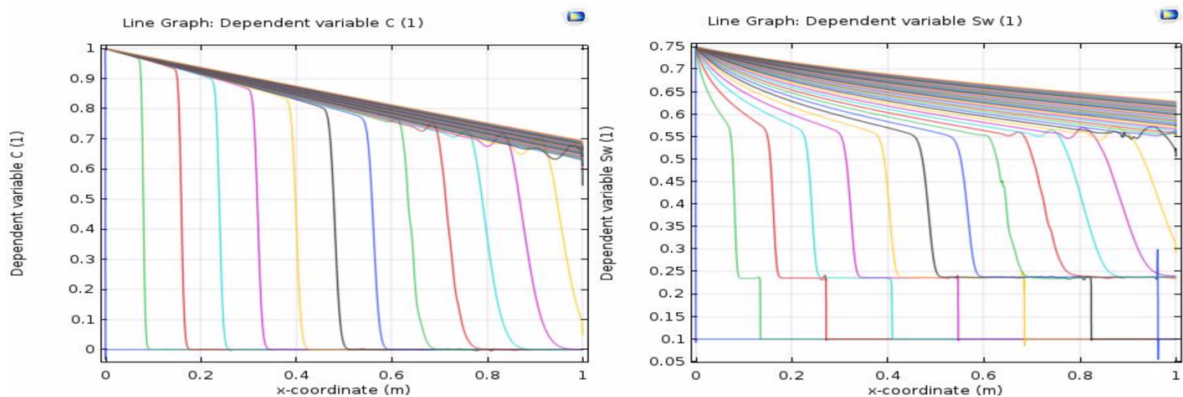


Figure 27: In case we increase the polymer concentration in polymer-solution, we can control effect of polymer entrapment. As it represented in water saturation and polymer concentration figures.

time t (s)	distance x(m)	Saturation (S_w)	Dimensionless Concentration	polymer viscosity (cP)	k_{rw} (relative water permeability)	k_{ro} (relative oil permeability)	Mobility Ratio
0,05	0,07	0,57	0,966	13,8145514	0,0946	0,065	0,799294879
0,1	0,146	0,564	0,932	13,3306056	0,0908	0,069	0,800138107
0,15	0,22	0,563	0,901	12,89067065	0,0908	0,069	0,8246827
0,2	0,3	0,557	0,865	12,38134625	0,087	0,075	0,829910519
0,25	0,378	0,555	0,833	11,93002785	0,087	0,076	0,859150949
0,3	0,456	0,551	0,803	11,50812585	0,0835	0,08	0,859960197

Table 7: Mobility ratio calculation through water saturation and polymer concentration, polymer viscosity, variation.

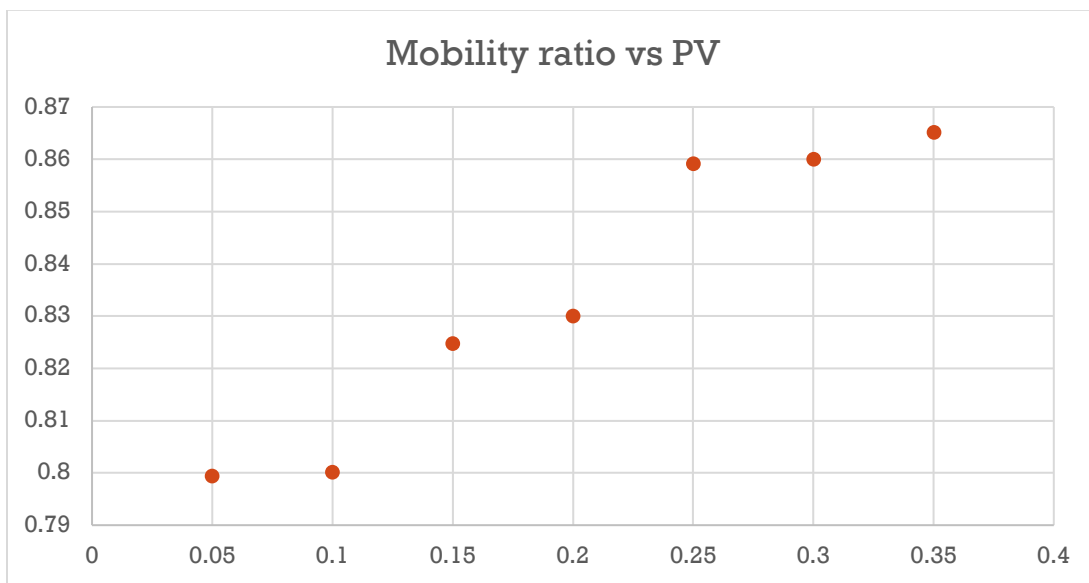


Figure 28: mobility ratio increasing during polymer flooding in case we have mechanical entrapment.

all in all, as it represents in Table 7, mechanical entrapment can increase the mobility ratio and as an outgrowth, it can influence dramatically the effectiveness of polymer flooding. Consequently, it is significant to investigate the impression of polymer entrapment in our simulation and reality in field-scale projects. Henceforward, mechanical entrapment can effect on the dispersion of polymer in porous media and also it can create viscous fingering by increasing mobility ratio. Accordingly, it is crucial to monitor viscous fingering in the 2D model. In the 1D

model, we can calculate the effect of polymer entrapment by observing the mobility ratio and acknowledging the non-constant filtration coefficient hypothesis.

Now to simulate viscous fingering in porous media in the situation in which we have a mobility ratio above 1, we demand to utilize the 2D model. According to the 1D model, the mobility ratio of the following model is above one. (meanwhile, we consider mobility ratio we merely examine the second saturation shock front which determines what we have on the left-hand side because the mobility ratio at the first saturation shock front entirely depends on the reservoir properties and principally oil viscosity and the relative permeability of water and oil).

Consequently, the subsequent model the mobility ratio computed 2.17, while water saturation before the polymer saturation shock front is 0.51. Accordingly, the water relative permeability is 0.0448 and the oil relative permeability is 0.0162. At the same time, the water saturation after polymer shock front is equal to 0.35, as a result, the relative permeability of water is 0.00508 and the relative permeability of oil is 0.4498. oil viscosity, in this case, considers 90 cP while water viscosity is 0.65 cP and polymer-solution viscosity is 2.6 cP. by using these data the mobility ratio at the polymer saturation shock front is 2.17. ($S_w^{before\ shock} = 0.51$, $S_w^{after\ shock} = 0.35$, $k_{rw}^{before} = 0.0448$, $k_{ro}^{before} = 0.0162$, $k_{rw}^{after\ polymer\ shock} = 0.00508$, $k_{ro}^{after} = 0.4498$, $\mu_w = 0.65\ cP$, $\mu_o = 90\ cP$, $m=2$ and $n=1$ in Equation 56, $M=2.17$).

In order to observe viscous fingering in porous media, we regularly demand to examine heterogeneity in the reservoir. Because to solve a partial differential equation through the finite element method, we consider the diffusion term. The diffusion term leads to stability in the shock saturation. which means that by decreasing Peclet number, we can eliminate all instability in all domains. Therefore, we consider heterogeneity in our simulation and v_{dp} (Dykstra-Parsons

coefficient)in our case, it is equal to 0.1 (v_{dp}). Therefore, this small amount of v_{dp} can verify viscous fingering nor channeling. (Ranganathan, 2012)

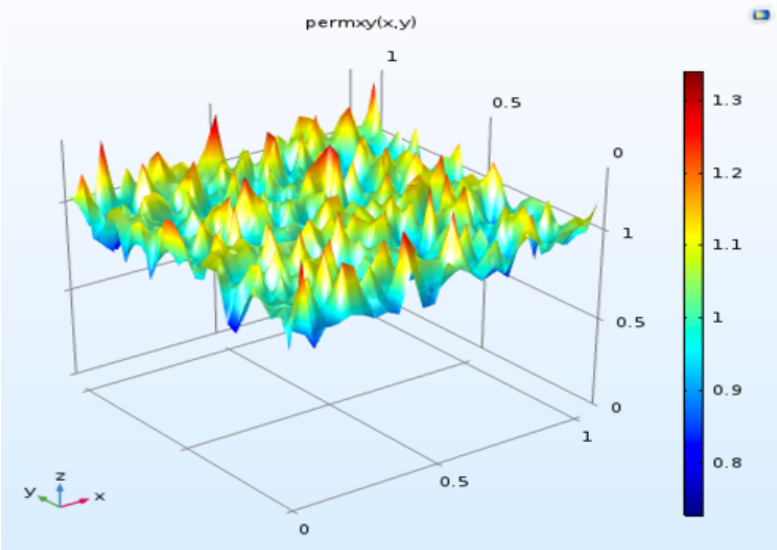
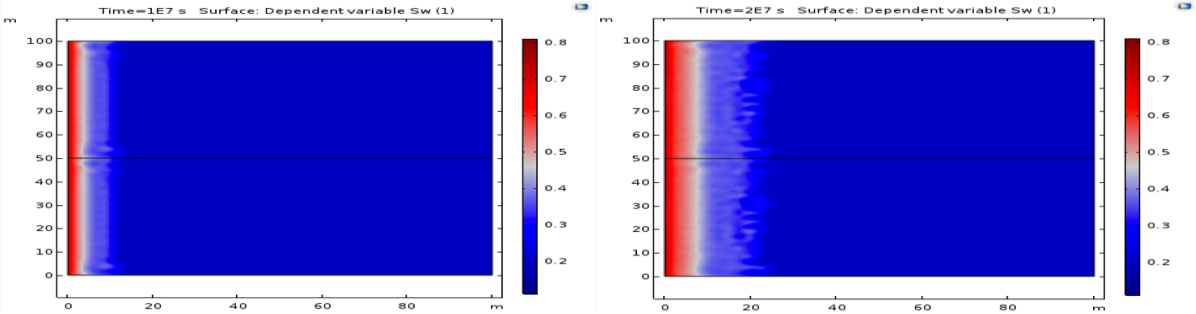


Figure 29: heterogeneity field which we used in 2D model. in order to monitor viscous fingering in our system better with considering the $v_{dp}=0.1$. which implies that we have viscous fingering nor channeling in our numerical simulation.



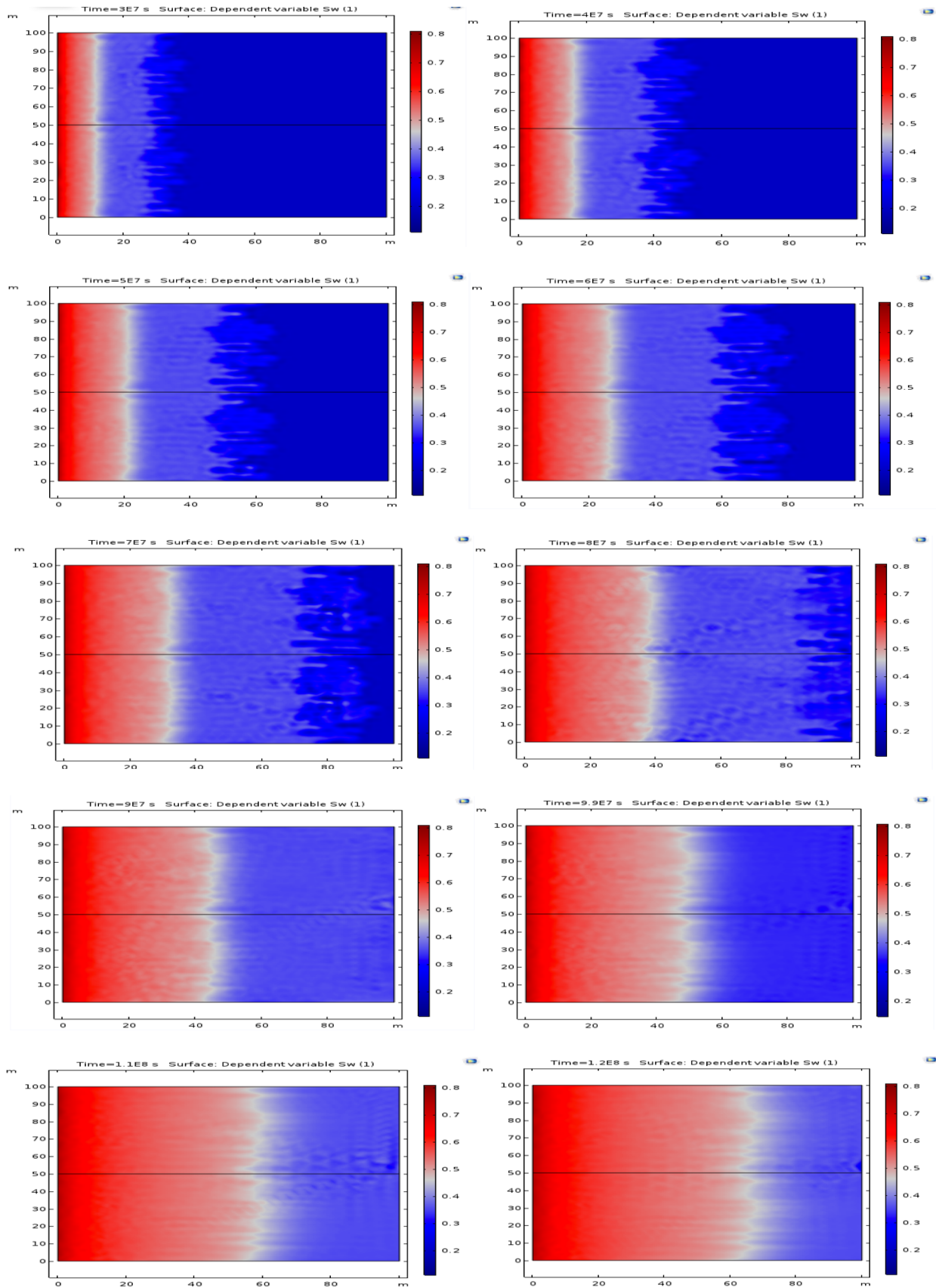


Figure 30: Polymer flooding in porous media in case we have mobility ratio of 2.17 in polymer saturation shock front. As represented here we can monitor instability in polymer shock front.

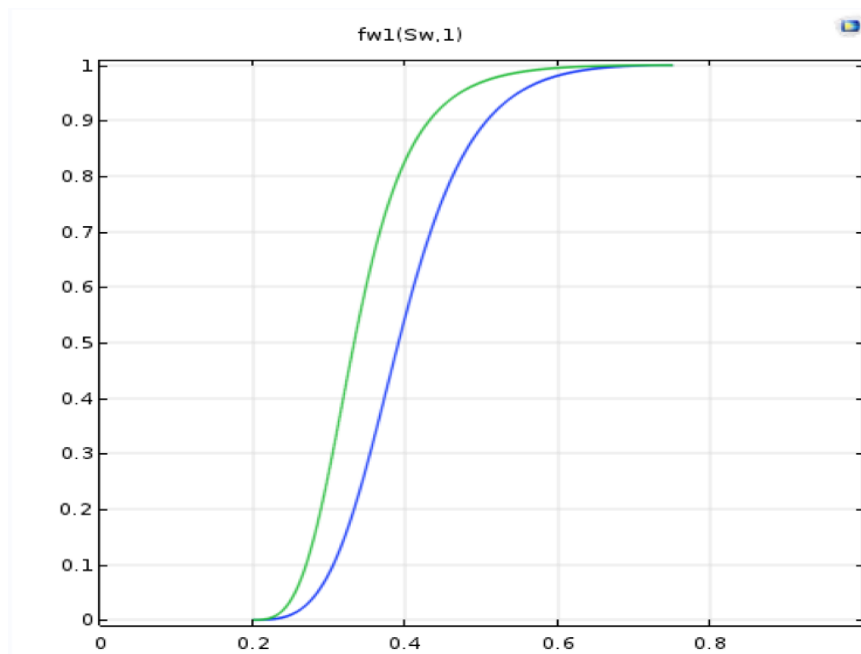
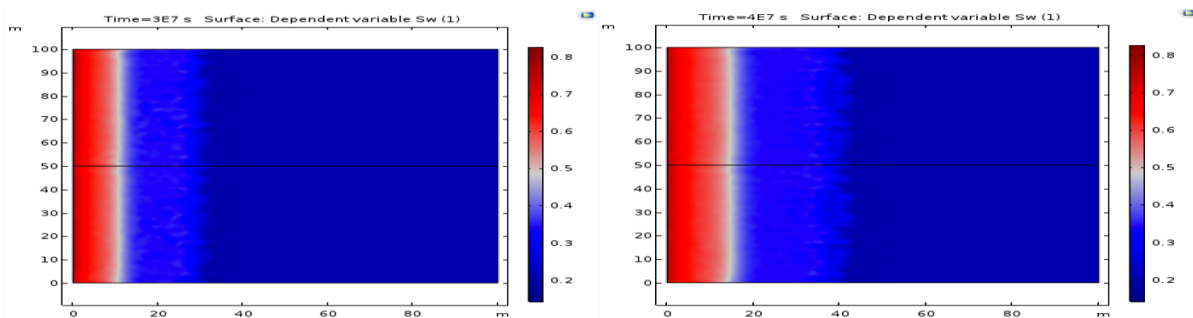


Figure 31: fractional flow as a function of water saturation. Blue curve represents the polymer flooding in porous media while the green line describes the water flooding. In chapter 2, I explained completely how we can obtain water saturation in upstream and downstream through fractional flow curves.



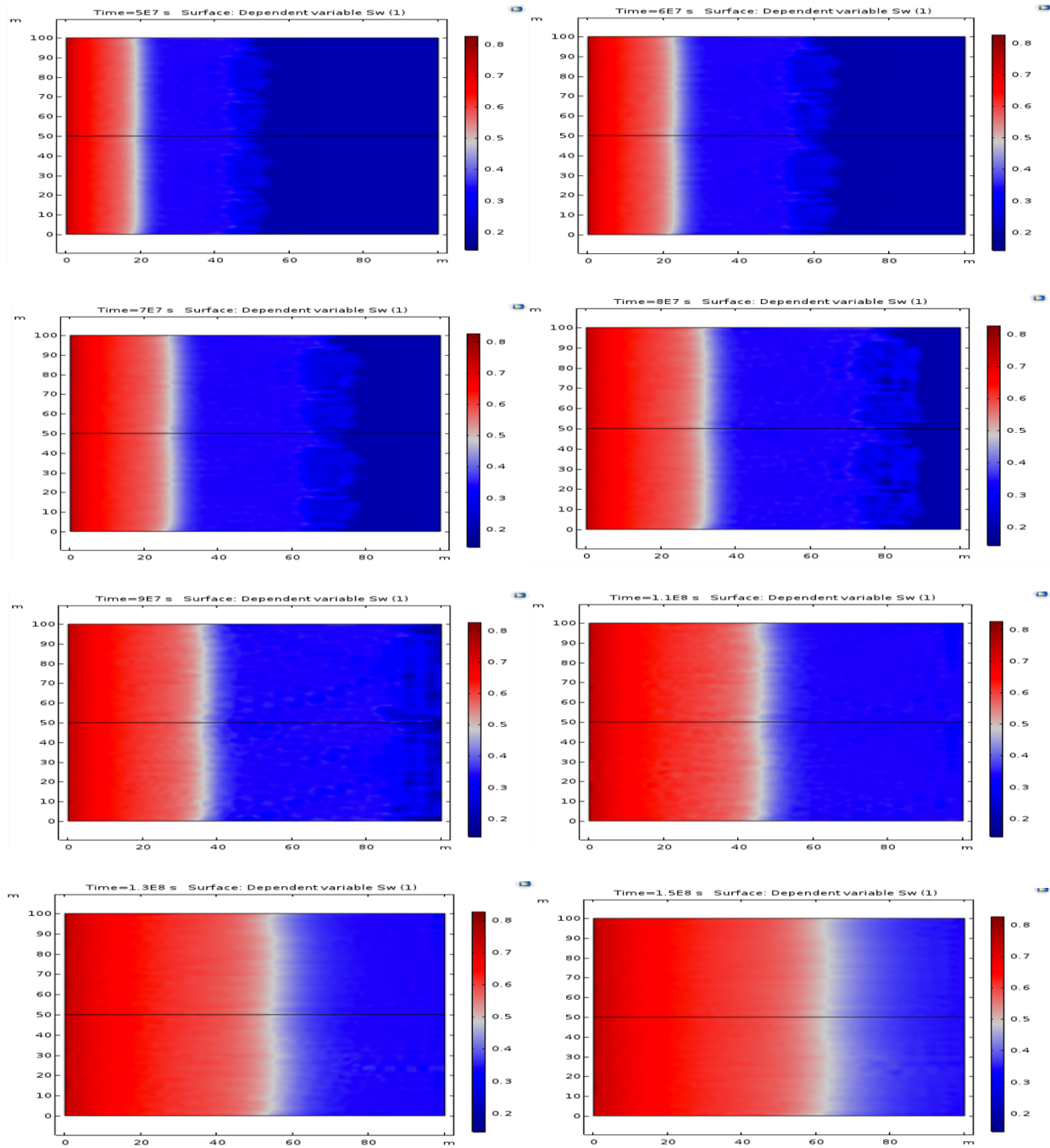
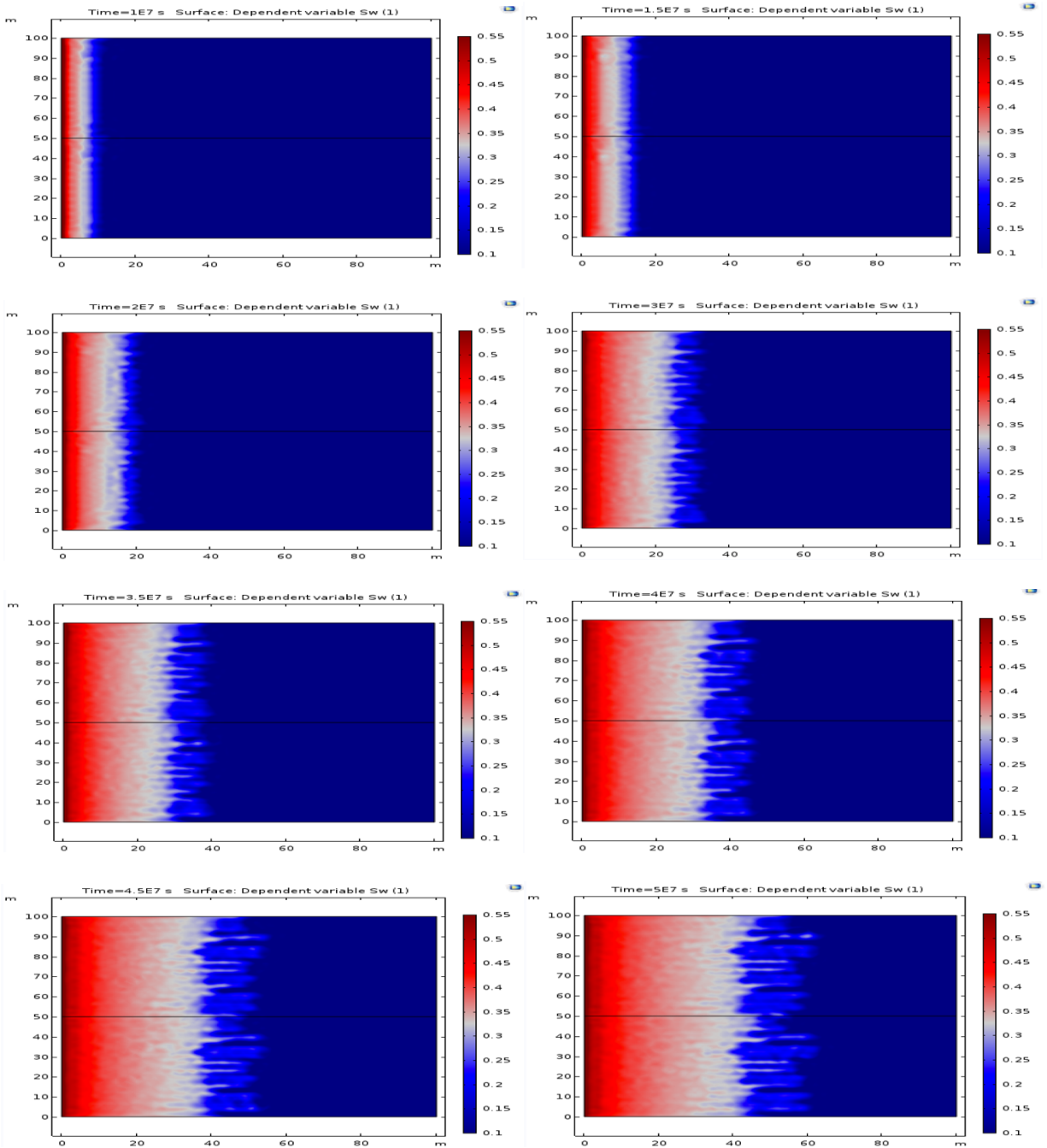


Figure 32: polymer propagation in porous media with the data at Table 2. In this case the polymer viscosity is 7.2 cP, which means that the mobility ratio is 1. Compare with Figure 30, where the mobility ratio is 2.17, we can show the effect of mobility ratio and instability of polymer shock front.

4.3 Effect of mechanical entrapment in 2D model:



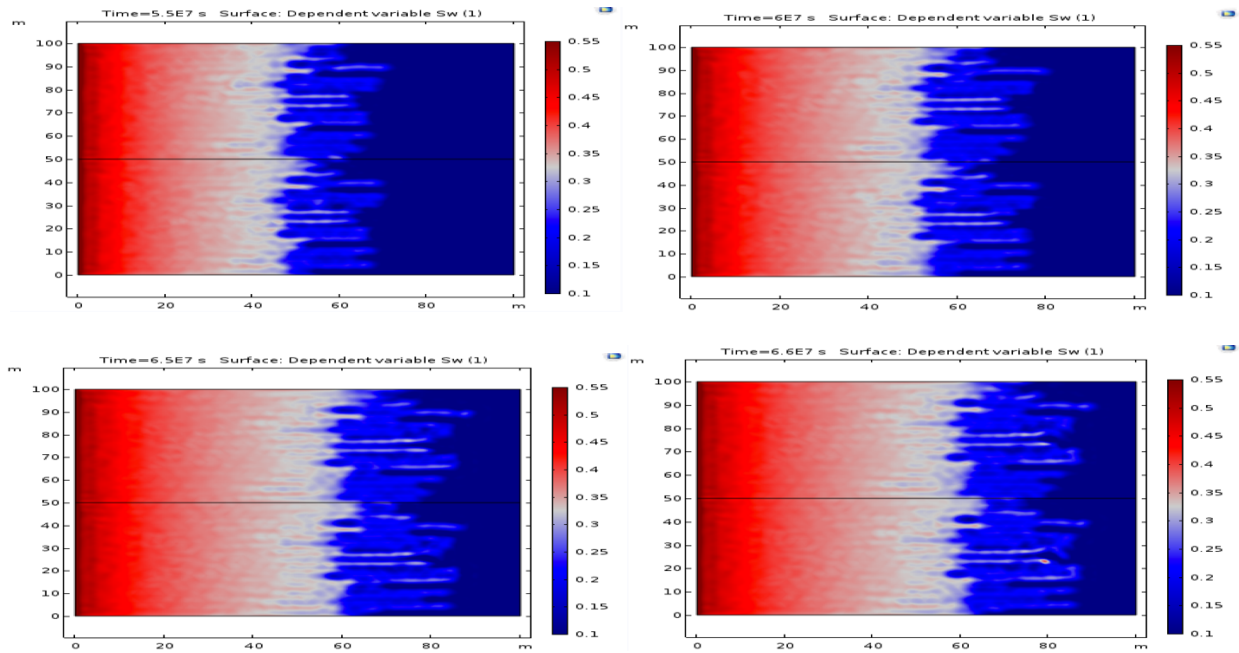


Figure 33: Using exactly the same data which we have in Table 3 but with considering mechanical entrapment. (on that case the without considering the mechanical entrapment, the mobility ratio was 1).

However in this figures we consider effect of mechanical entrapment and as it represented we have

instability in polymer shock front. ($\lambda_0 = 0.438 \frac{1}{m}$, $\sigma_{max} = 0.695$, $Peclet=9e10$),

Chapter 5 *Conclusion*

Polymer combined with the oil to enhance the viscosity of the water to improve the sweep efficiency in a reservoir. Raising the viscosity of the polymer, the mobility ratio diminishes, which assists in circumventing viscous fingering phenomena and instability on the polymer saturation shock front. In this thesis, I investigate the influence of mechanical entrapment and adsorption on the performance of polymer flooding in porous media. Subsequently, the small volume of the polymer can increase the viscosity of the water dramatically. Nevertheless, it is crucial that this polymer propagates in the reservoir properly. It implies that all polymer should cross through the pore throats of the porous media, which explicates the importance of the size of the polymer. Nonetheless, generally in the industry, the mean size of the polymer announced. Nevertheless, all the polymer does not have the same size and the polymer size distribution is crucial criteria to investigate the polymer propagation. Usually, due to the limitation which we have in well-injectivity, it is more desirable to utilize polymer with more size cause tend to the large polymer can execute our solution extra viscous. Notwithstanding, experimentation determines that as much as polymer length grows, degradation increases. Moreover, the polymer can be trapped in porous media in case the size of the polymer is more than the smallest pore size. Accordingly, the pore size distribution and polymer size variation play an influential role in polymer propagation and mechanical entrapment. Mechanical entrapment mostly diminishes the effective permeability and reducing the polymer concentration in the polymer saturation shock front. generally, the mechanical entrapment will display with filtration approach, in this thesis we examine the non-constant filtration coefficient to model polymer retention in porous media. Adsorption of the polymer additionally is a different serious concern that can influence considerably in polymer propagation. The surface charge of rock, particularly in the clay rock, leads to having a reaction between the polymer and surface of the rock. the retardation of polymer flow due to polymer adsorption is one of the most remarkable consequences that can transpire through polymer EOR.

Adsorption can also change the effective permeability of the reservoir. Entirely both mechanical entrapment and adsorption of the polymer can decrease the effective permeability of the reservoir. Nevertheless, the adsorption chiefly makes a postponement in polymer propagation and does not affect polymer concentration in the saturation shock front. While mechanical entrapment essentially acts on polymer concentration. In this research, the effect of polymer entrapment is represented in both 1D and 2D model. The instability monitor in case of the mobility ratio increase above one. The mobility ratio during polymer front with respecting the mechanical entrapment increases constantly. Because polymer concentration diminishes steadily. The result in 1D also compared with both the analytical solution and experimental data. In the analytical solution, the diffusion coefficient is considered negligible. Nevertheless, experimental data explicates diffusion presents in laboratory data. Applying numerical simulation, we describe how diffusion term can influence our model. All in all, this thesis investigates the influence of mechanical entrapment in the concentration of polymer, polymer propagation, water saturation, pressure, and effective permeability.

Chapter 6 Bibliography

Ahmed, T. (2012). *Advanced Reservoir Management and Engineering (Second Edition)*. ScienceDirect.

Al-Hajri, S. (2018). an overview on polymer retention in porous media. *Energy Journal* .

Baviere, M. (1995). Improvement of efficiency/cost ratio of Chemical eor processes by using surfactants, polymer, and alkalis in combination. *SPE*.

Bouquet, S. (2017). Characterization of viscous unstable flow in porous media at pilot scale. application to heavy oil polymer flooding . *19th European symposium on improved oil recovery* . Stavenger : EAGE.

Chorin, A. J. (1983). The instability of fronts in a porous medium. *Communications in Mathematical Physics*, 103-116.

Clark, D. T. (1982). Advances in ESCA applied to polymer characterization. *Pure and Applied Chemistry* .

Dake. (n.d.). *Fundamentals of Reservoir Engineering*. Elsevier, N. Y (1978).

Daleel Prteoleum L.L.C. (n.d.). Daleel Petroleum L.L.C.

Delamaide, E. (2014). Polymer flooding of heavy oil- from screening to full-field extension. *SPE heavy and extra heavy oil conference* (pp. 24-26). Medellin, Colombia : SPE.

Dunstan, D. E. (2019). The viscosity-radius relationship for concentrated polymer solutions. *Nature* .

Fanchi, J. R. (2002). *Shared Earth Modeling* . Elsevier Inc.

Farajzadeh, R. (2019). Insights into design of mobility control for chemical enhanced oil recovery. *energy report* .

- Gopferich, A. (1996). Mechanisms of polymer degradation and erosion . *Biomaterials* , 103-114 .
- Hosseini, S. J. (2019). Experimental study of polymer injection enhanced oil recovery in homogeneous and heterogeneous porous media using glass-type micromodels . *Journal of petroleum exploration and production technologies*, 627–637.
- Karnanda, W. (2012). Effect of temperature, pressure, salinity, and surfactant concentration on IFT for surfactant flooding optimization . *Arabian Journal of Geosciences*.
- Kleppe, J. (2009). *Surfactant flooding as a possible for the Norne E-Segment*. NTNU .
- Lake, L. W. (2014). *Fundamentals of Enhanced oil recovery*. SPE.
- Lotfollahi, m. (2015). Mechanistic Simulation of Polymer Injectivity in Field Tests. *SPE asia pacific enhanced oil recovery conference*. Kuala lampur: SPE.
- Lotfollahi, M. (2016). Mechanistic simulation of polymer injectivity in field tests . *SPE Journal* .
- Moreno, F. V. (2016). Modeling and Simulation of Laboratory-Scale Polymer Flooding. *International Journal of Engineering and Technology IJET*.
- Needham, R. B. (1987). Polymer flooding review. *Journal of petroleum technology* .
- Paul, G. W. (1982). A Simplified Predictive Model for Micellar-Polymer Flooding . *SPE California Regional Meeting, 24-26 March, San Francisco, California*. California : SPE.
- Pope, G. A. (1980). The Application of fractional flow theory to Enhanced oil recovery . *SPE Journal* .
- Prasad, R. G. (2018). Enhanced Oil Recovery by using Polymer Flooding in Oil and Gas Industry in Tertiary Recovery Process. *International Journal for Research in Applied Science & Engineering Technology (IJRASET)*.

- Ranganathan, P. (2012). Numerical Simulation of Natural Convection in Heterogeneous Porous media for CO₂ Geological Storage . *Transp Porous Med.*
- Seright, R. (2010). Potential for polymer flooding reservoirs with viscose oils . *SPE reservoir evaluation and engineering* .
- Skauge, A. (2018). Impact of Mechanical Degradation on Polymer Injectivity in Porous Media. *Polymers.*
- Sorbie, K. (1991). *Polymer-Improved Oil Recovery.*
- Speight, J. G. (2016). *Introduction to Enhanced Recovery Methods for heavy oil and Tar Sands.*
- Stosur, G. (2003). The alphabet soup of IOR,EOR and AOR, effective communication requires a definition of terms. *SPE international improved oil recovery conference in asia pacific.*
- Thomas, S. (2008). Enhanced oil recovery- an overview. *IFP intenational conference.* Paris, France: oil and gas science and technology.
- UNSW, School of material science and engineering . (2013). Retrieved from <http://www.materials.unsw.edu.au/tutorials/online-tutorials/2-polymer-chains>.
- Vermolen, E. C. (2014). Low-Salinity polymer flooding: improving polymer flooding technical feasibility and economics by using low-salinity make-up brine. *International Petroleum Technology Conference* . Doha, Qatar : International Petroleum Technology Conference .
- W.B.Gogarty. (1970). Mobility Control Design for Miscible-Type Waterfloods Using Micellar Solutions. *Journal of Petroleum Technology* 22(2):141-147, DOI: 10.2118/1847-E-PA, 141-147.
- Wei, B. (2014). Oil displacement mechanisms of viscoelastic polymers in enhanced oil recovery (EOR): a review. *journal of petroleum exploration and production technology* , 113-121.
- Zhang, G. (2014). Effect of Concentration on HPAM Retention in Porous Media . *SPE Journal.*

Zitha. (1998). Bridging-Adsorption of Flexible Polymers in Low Permeability Porous Media . *SPE Production & Facilities*, 15-20.